

AD-A121 985

HYDRODYNAMIC NOISE AND SURFACE COMPLIANCE(U) NAVAL
UNDERWATER SYSTEMS CENTER NEW LONDON CT NEW LONDON LAB
W A WINKLE ET AL. 08 SEP 82 NUSC-TD-6607

1/1

UNCLASSIFIED

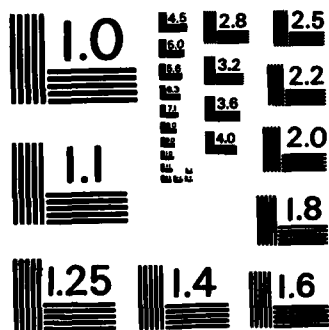
F/G 20/1

NL

END

FILED

2140



MICROCOPY RESOLUTION TEST CHART
NATIONAL BUREAU OF STANDARDS-1963-A

2

NUSC Technical Document 6607
8 September 1982

AD A121905

Hydrodynamic Noise and Surface Compliance

William A. Von Winkle
Naval Underwater Systems Center

James Fitzgerald
B-K Dynamics, Inc.

William M. Carey
Naval Research Laboratory

Henry P. Bakewell, Jr.
MAR, Inc.



NOV 26 1982

A

Naval Underwater Systems Center
Newport, Rhode Island / New London, Connecticut

Approved for public release; distribution unlimited.

82 11 26 150

WING FILE COPY

Preface

This document was prepared under Project No. 710X11.

Reviewed and Approved: 8 September 1982



W. A. Von Winkle

Associate Technical Director for Technology

**Any inquiries concerning this document should be referred
to Dr. W. A. Von Winkle (Code 10),
Naval Underwater Systems Center, New London Laboratory,
New London, Connecticut 06320**

| REPORT DOCUMENTATION PAGE | | READ INSTRUCTIONS BEFORE COMPLETING FORM |
|---|---|---|
| 1. REPORT NUMBER TD 6607 | 2. GOVT ACCESSION NO. AD-A222 905 | 3. RECIPIENT'S CATALOG NUMBER |
| 4. TITLE (and Subtitle) HYDRODYNAMIC NOISE AND SURFACE COMPLIANCE | | 5. TYPE OF REPORT & PERIOD COVERED |
| | | 6. PERFORMING ORG. REPORT NUMBER |
| 7. AUTHOR(s) William A. Von Winkle (NUSC), James Fitzgerald (B-K Dynamics, Inc.), William M. Carey (NRL), and Henry Bakewell, Jr. (MAR, Inc.) | | 8. CONTRACT OR GRANT NUMBER(s) |
| 9. PERFORMING ORGANIZATION NAME AND ADDRESS Naval Underwater Systems Center New London Laboratory New London, CT 06320 | | 10. PROGRAM ELEMENT, PROJECT, TASK AREA & WORK UNIT NUMBERS 710X11 |
| 11. CONTROLLING OFFICE NAME AND ADDRESS | | 12. REPORT DATE 8 September 1982 |
| | | 13. NUMBER OF PAGES 50 |
| 14. MONITORING AGENCY NAME & ADDRESS (if different from Controlling Office) | | 15. SECURITY CLASS. (of this report) UNCLASSIFIED |
| | | 15a. DECLASSIFICATION / DOWNGRADING SCHEDULE |
| 16. DISTRIBUTION STATEMENT (of this Report) Approved for public release; distribution unlimited | | |
| 17. DISTRIBUTION STATEMENT (of the abstract entered in Block 20, if different from Report) | | |
| 18. SUPPLEMENTARY NOTES | | |
| 19. KEY WORDS (Continue on reverse side if necessary and identify by block number) Complex Surface Compliance Turbulent Boundary Layer (TBL) Flow Noise Wall Pressure Fluctuations (pseudosound) Hydrodynamic Noise Mammalian Tissues | | |
| 20. ABSTRACT (Continue on reverse side if necessary and identify by block number) Over the past 25 years investigations of turbulent boundary layer (TBL) noise have concentrated on measuring the spectral and cross-spectral properties of wall pressure fluctuations, i.e., pseudosound (D. Blokhintzev, "The Acoustics of an Inhomogeneous Moving Medium," NACA Technical Memorandum No. 1399 (1966).), utilizing turbulent flow on flat plates and in pipes. The pseudosonic pressure fluctuations and their induced vibrations are referred to generically as flow noise, which is currently considered the limiting factor in sonar performance. Proper design of sensors, the (Over) | | |

20. (Cont'd)

use of arrays, the reduction in the sensitivity to flow-induced vibrations have all decreased this noise. The measurement of the TBL pressure fluctuation requires determining the spectral properties. The normalized fluctuation power spectra versus Strouhal number is known to be constant out to a nondimensional frequency $f\delta^*/U$ of 0.1; thereafter, for point-like transducers, the level decreases at a rate between 9 and 12 dB per octave for noninteracting surfaces. Flexible surfaces are shown to influence the shapes of these spectra, and data on the Kramer surface (M. Kramer, "Boundary Layer Stabilization Distributed Damping," Journal of the Acoustical Society of America, vol. 24, no. 6, 1957)) show a decrease in the spectral level and slope. Earlier experimentalists concentrated on the measurement of longitudinal and transverse correlative properties of the TBL pressure fluctuations. → This document discusses the role of surface compliance on hydrodynamic noise and is based on a review of theoretical and experimental flow-noise investigations. Basic flow-noise theories are discussed in light of compliant surface boundary conditions. A comprehensive review of the experimental results of compliant surface flow-noise experiments is presented. Surface compliance can effect the measured noise; however, the compliance of the surfaces used in previous experiments was not adequately described. Consequently, results varied and showed a marked, but undefined, temperature dependence. The characterization of the complex surface compliance is discussed, including effects of frequency and temperature. A method that characterizes surface compliance is denoted and used to measure the properties of several mammalian tissues. Then a discussion and a comparison of these results to the wavenumber spectra data follows. An experimental investigation of the effect of surface compliance on the hydrodynamic noise is proposed by means of measurement of material properties, measurement of wall pressure fluctuation spectra, holographic representation of the surface displacement, and characterization of the TBL boundary layer to determine the magnitude and role of complex surface compliance of the TBL and its flow noise. ←

TABLE OF CONTENTS

| | Page |
|---|------|
| LIST OF ILLUSTRATIONS | ii |
| LIST OF TABLES | ii |
| GLOSSARY | iii |
| INTRODUCTION | 1 |
| A BRIEF THEORETICAL OVERVIEW | 2 |
| A REVIEW OF EXPERIMENTAL WORK | 4 |
| Mean Square Pressure Measurement | 5 |
| Nondimensional Wall Press Spectra | 5 |
| Convection Velocities | 9 |
| Cross-Spectral Densities | 9 |
| COMPLIANT SURFACE EXPERIMENTS | 17 |
| PRELIMINARY MATERIAL MEASUREMENT | 23 |
| PROPOSED EXPERIMENT | 28 |
| Material Measurement Requirements | 28 |
| Flow Experiment | 28 |
| SUMMARY | 35 |
| REFERENCES | 37 |



A

LIST OF ILLUSTRATIONS

| Figure | | Page |
|--------|--|------|
| 1 | Dimensionless Wall Pressure Spectra As a Function of Dimensionless Frequency | 8 |
| 2 | Ratio of Convection Velocity to Centerline Velocity As a Function of Frequency | 10 |
| 3 | Ratio of Convection Velocity to Centerline Velocity As a Function of Reynolds Number | 11 |
| 4 | Dependence of Measured rms Wall Pressure Fluctuations Upon the Dimensionless Transducer Diameter | 12 |
| 5 | Magnitude of the Normalized Longitudinal Cross-Spectral Density . | 14 |
| 6 | Magnitude of the Normalized Lateral Cross-Spectral Density..... | 15 |
| 7 | Longitudinal Space-Time Correlation of the Wall Pressure As a Function of Nondimensional Transducer Separation, X_1/δ^* , and Time Delay $\tau U_\infty/\delta^*$ | 16 |
| 8 | Typical Longitudinal Wavenumber Spectrum for Constant Frequency ω_0 Showing Location of Nearfield and Radiated Noise Components..... | 18 |
| 9 | Noise Investigations..... | 20 |
| 10 | Broadband Sound Pressure Level As a Function of Vehicle Velocity Measured With Hydrophone No. 2..... | 21 |
| 11 | Dimensional Wall Pressure Spectrum As a Function of Frequency Measured With Hydrophone No. 2..... | 22 |
| 12 | Complex Shear Compliance As a Function of Frequency for Selected Materials | 25 |
| 13 | Shear Loss Tangent As a Function of Frequency for Selected Materials | 26 |
| 14 | Acoustic Water Tunnel..... | 30 |
| 15 | Rectangular Test Section Assembly | 31 |
| 16 | Spectral Density--Background Noise Versus Flow Noise..... | 32 |
| 17 | Planned Compliant Surface Experiment..... | 33 |

LIST OF TABLES

| Table | | Page |
|-------|---|------|
| 1 | Summary of Root Mean Square Pressure Measurements | 6 |

GLOSSARY

| | |
|---------------------------|---|
| BBF | Beef-belly fat |
| FFT | Fast Fourier transform |
| HON | Honey |
| LDV | Laser Doppler velocimeter |
| NRS | Natural rubber stock |
| NUSC | Naval Underwater Systems Center |
| PBF | Pork-belly fat |
| PUR | Polyurethane rubber |
| PVC | Polyvinylchloride |
| PVG | Polyvinylchloride (10%) Dimethylthianthrene (90%) gel |
| rms | Root mean square |
| SPL | Sound pressure level |
| TBL | Turbulent boundary layer |
| A, B, C | Corcos Functions |
| C_f | Coefficient of friction |
| C_o | Sonic velocity (m/s) |
| C_p | Pressure coefficient |
| G | Shear modulus |
| J | Shear compliance |
| P | Pressure (N/m ²) |
| Re | Momentum thickness Reynolds number |
| P_{RMS} | Root mean square pressure |
| S_o | Surface area (m ²) |
| U_∞ | Free stream velocity (m/s) |
| U_c | Convection velocity (m/s) |
| V_o | Volume (m ³) |
| V | Velocity (m/s) |
| d | Spatial distance (m) |
| f | Force (N) |
| f | Frequency |
| i, j | Subscripts |
| k | Wavenumber |
| q | Mass per unit volume source term (kg/m ³) |
| $q = 1/2 \rho U_\infty^2$ | Dynamic pressure |
| r | Radial coordinate |
| t | Time |
| w | Wall subscript |
| x | Spatial coordinate |
| $\delta(x)$ | Dirac delta function |
| δ^* | Displacement boundary layer thickness |
| η | Coefficient of bulk viscosity |
| η | Spatial separation variable |

GLOSSARY (Cont'd)

| | |
|--------------------------------------|--------------------------------------|
| κ | Compressibility |
| $\lambda = 2\pi/k = 2\pi C_o/\omega$ | Wavelength |
| μ | Coefficient of viscosity |
| ν | Kinematic viscosity |
| θ | Momentum thickness of boundary layer |
| ξ | Spatial separation variable |
| ρ | Density |
| τ | Time shift |
| τ_{ij} | Shear stress tensor |
| τ_w | Wall shear stress |
| Γ | Cross-spectral density |
| ϕ | Spectral density |
| $\omega = 2\pi f$ | Angular frequency |

HYDRODYNAMIC NOISE AND SURFACE COMPLIANCE

INTRODUCTION

In the general sense, the term "flow noise" attributes the self-noise of a sonar transducer to the nearfield turbulent boundary layer (TBL) flow noise (pseudosound),¹ the flow-induced vibrations of the sensor and its surrounding structure, and the acoustic component that is radiated to distant parts of the fluid. At operational ship speeds, surface ship, submarine, and towed array sonar systems are subject to potential performance limitations due to the noise from the turbulent flow. Major advances in the reduction of self-noise have been achieved, and further reductions may be possible if the nature of the TBL and its wall pressure fluctuations can be altered.

The dolphin is characterized by a surface that is considered to have low hydrodynamic drag, low flow noise, and an ability to delay the onset of TBL. These effects may be a result of the viscoelastic properties of the blubber. Proper selection of a viscoelastic surface for investigation that includes the properties of the dolphin's blubber requires knowledge of the material's temperature and frequency dependent viscoelastic properties. Whether such a compliant surface will significantly reduce the self-noise depends on the effects of surface compliance in the production of TBL flow noise. Thus, the basic questions that arise are

How does a compliant surface affect the TBL
and the production of flow noise?

What is the potential reduction in noise that can be
expected with a compliant surface?

What is the best way to characterize the
compliance of the surface?

Can a carefully controlled laboratory experiment
be conducted to demonstrate the differences between
rigid and compliant surfaces and the production of
flow noise?

These questions constitute the statement of the problem considered here.

This document includes a brief overview of the theoretical considerations necessary to describe the effect of surface compliance on flow noise and a review of previous measurements on rigid, flexible, and compliant surfaces. In addition, a method is discussed that will characterize viscoelastic moduli of materials such as

dolphin's blubber. An experiment is also suggested to determine the role of surface compliance in drag and noise reduction. This document's approach differs from previous investigations, such as the work of Kramer,² insofar as the selection of materials will be based on knowledge of the materials' properties supported by measurements.

A BRIEF THEORETICAL OVERVIEW

The recognition of noise production by turbulent flow had its origin in the nineteenth century and, not surprisingly, it was investigated by Rayleigh. However, a theoretical description of the noise production is difficult due to the complex nature of the turbulent flow field. More recently, the distinction between the pseudosound field on the surface and the radiated acoustic problem has been investigated theoretically by several investigators. The radiated sound field has been treated most notably by Lighthill,^{3,4} Ffowcs-Williams,⁵⁻⁷ and Morse and Ingard.⁸ Ffowcs-Williams⁷ excellent review identifies five distinctly different theoretical efforts to describe the radiated sound. These are Lighthill's acoustic analogy, Liepmann's boundary layer fluctuation, Phillip's work on supersonics, the matched asymptotic expansion technique developed independently by several investigators, and finally Morefy's treatment of the energy balance equations in acoustics.

The Lighthill technique^{3,4} adopted by many including Ffowcs-Williams⁵⁻⁷ is based on the acoustic wave equation as derived from the principles of conservation of mass and momentum, with the source term $f(r,t)$ included on the right-hand side. Thus, one finds

$$\frac{1}{C_0^2} \frac{\partial^2 P}{\partial t^2} - \frac{\partial^2 P}{\partial x_i^2} = \frac{\partial q}{\partial t} - \frac{\partial f_i}{\partial x_i} + \frac{\partial \tau_{ij}}{\partial x_i \partial x_j} = +f(r,t),$$

where the summation convention applies; C_0 is the acoustic propagation velocity (m/s) and P is the acoustic pressure (N/m²). The right-hand side of this form of the wave equation contains the monopole, dipole, and quadrupole source terms. Lighthill noted that the first term represents the mass fluctuation in a fixed region (kg/m³/s). Since mass is not created, this term can be shown to yield the volume velocity source term, a monopole. The second term represents the divergence of the external fluctuating forces $f_i(r,t)$ in Newtons, which represents a variation in momentum; this term represents a dipole term. The final term represents the gradient of the turbulent shear stress; in this form it represents a variation in momentum efflux from a fixed region. The quadrupole nature of this term is readily observed. The first two terms require a boundary while the third may be valid in boundary-free regions. The Lighthill stress tensor is written as follows:

$$\tau_{ij} = \rho v_i v_j + (P_{ij} - C_0^2 \rho \delta_{ij}).$$

The first term, $\rho v_i v_j$, represents the fluctuating shear stress associated with the turbulent flow, whereas $P_{ij} - C_0^2 \rho \delta_{ij}$, represents the fluid stress tensor, including viscous and heat conduction terms. Lighthill observed that only the first term of the

stress tensor was pertinent to the turbulent flow in the absence of boundaries. Fourier transforming both sides for the wave equation yields

$$\nabla^2 p_\omega + k^2 p_\omega = -f_\omega(r),$$

the solution of which can be obtained by the Green's function technique as

$$p_\omega(r) = \int_{V_0} dV_0 f_\omega(r_0) G(r, r_0) + \int_{S_0} dS_0 \left[G(r, r_0) \frac{\partial p_\omega(r_0)}{\partial n_0} - p_\omega(r_0) \frac{\partial G(r, r_0)}{\partial n_0} \right],$$

where n_0 is the coordinate direction normal to the surface S_0 .

Most theoretical solutions to the above equation describing the radiation from turbulence assume outward propagating waves without surfaces that reflect, scatter, or diffract. In this case, the surface integral vanishes, leaving the description of the radiated pressure wave dependent solely on the form of $f_\omega(r)$. In general, a qualitative argument can be made for the form of $f_\omega(r)$. A local fluctuation in a fluid will produce a local pressure variation of the order of V^2 that acts as a monopole source of sound and gives rise to a radiated power proportional to the fourth power of the velocity fluctuation. In the absence of boundaries and net mass transfer into and out of our volume, the monopole contribution from the volume integral will be zero. Likewise, two point sources of opposite signs separated by a short distance behave as a dipole and the pressure is d/λ times the monopole pressure, or the power is $[(d/\lambda)^2 = V^2/c^2]$ times the monopole power. Thus, a variation with the sixth power is realized. The presence of the dipole requires a finite exchange of momentum. In the absence of external forces or boundaries, there will be no net momentum transfer, and the volume integral of dipole terms will be zero. Finally, in the absence of mass transfer into the volume and no net momentum transfer, the remaining source term is the quadrupole term. The acoustic power from the quadrupoles varies with velocity to the eighth power. In Lighthill's model^{3,4} there is no net mass or divergence force transfer, so that the dipole and monopole contributions are zero. Therefore, neglecting heat conduction and shear stress effects, the source simply becomes the second derivative of the turbulent stress tensor, as shown previously:

$$\frac{\partial^2 \tau_{ij}}{\partial x_i \partial x_j} = \frac{\partial^2 \rho v_i v_j}{\partial x_i \partial x_j}.$$

Thus, Lighthill's result^{3,4} predicts the quadrupole character of the noise.

Ffowcs-Williams⁶ adopted the Lighthill technique^{3,4} but allowed a surface to be present. He discusses the roles of the rigid surface, a pressure release surface, and a compliant surface on the radiation of sound. His conclusion that the rigid surface acts as a sounding board increasing the sound production is in agreement with the results of Powell⁹ and Curle¹⁰ that the pressure release surface does not enhance the sound production. He concluded that for small deformations of a compliant surface no increased radiation field would be observed but, rather, the result would be a decreased magnitude of the surface images.

The boundary condition for the rigid surface is simply stated by the requirement that the particle velocity vanish at the surface; i.e., the $\partial P_\omega(r_0)/\partial n_0$ terms equal zero. However, the pressure release surface requires that the pressure, $P_\omega(r_0)$, equals zero. For the real viscoelastic surface, continuity of pressure and velocity at the interface is required. Inclusion of the viscoelastic shear moduli also requires consideration of tangential balances; a problem apparently not yet solved.

The relation of radiated noise to the dynamic hydrodynamic pressure is evident if the wave equation before the acoustic approximation is written as follows:

$$\rho \kappa \frac{\partial^2 p}{\partial t^2} - \sum_{i,j} \frac{\partial^2 \rho v_i v_j}{\partial x_i \partial x_j} = \nabla^2 p$$

If the compressibility is considered to be zero, then the pressure field is described by

$$\nabla^2 p = - \sum_{i,j} \frac{\partial^2 \rho v_i v_j}{\partial x_i \partial x_j}$$

Thus, the pressure fluctuations are of the order ρV_j^2 i.e., the hydrodynamic pressure field. In a moving compressible fluid, therefore, there are both the pseudosonic and the acoustic radiated pressure fields.

The discussion on the theoretical description of the role of surface compliance in TBL flow noise can now be summarized by the requirement of a solution to the previously described surface integral with realistic boundary conditions. Ffowcs-William^{5,6} has attempted to solve this problem for the acoustic field when the boundary does not interfere with the flow. Several authors have tried to describe the hydrodynamic problem as a point load on an elastic structure and, thereby, have explained the resultant flow-induced vibration. A realistic treatment of the pseudosonic problem has not been realized and, thus, there is no theoretical model with which to assess the role of compliance.

The pseudosonic field has been treated by Kraichnan¹¹⁻¹³ who showed that the wall pressure fluctuations were influenced by the mean velocity gradient. Batchelor¹⁴ has also treated the case of this pseudosound within isotropic turbulence. However, in all the work based on Kraichnan's results, the pseudosonic pressure level was determined to be proportional to the square of velocity and to have space and time properties similar to the turbulence itself.

A REVIEW OF EXPERIMENTAL WORK

Boundary layer flow noise investigations have resulted in the measurement of the fundamental properties of wall pressure fluctuations and pseudosound from TBL flows on rigid flat plates, pipes, and bodies of revolution. Several excellent reviews by Fitzpatrick and Strasberg,¹⁵ Haddad and Skudrzyk,¹⁶ Willmarth,¹⁷ and

Ross¹⁸ are available on this subject. This article consolidates and presents a summary of experimental evidence for turbulent flow on both rigid and compliant surfaces. It draws heavily on previous experiments and reviews in order to present a concise yet thorough overview of the wall pressure fluctuation measurements.

MEAN SQUARE PRESSURE MEASUREMENT

The mean square pressure has been measured on two-dimensional flat plates,¹⁹⁻²⁶ in fully developed pipe flow,²⁷⁻³⁴ and on solid bodies of revolution.^{21,22,35-37} These data are summarized in table 1 and show that the root mean square pressure (P_{RMS}) is between 0.97 to 3.24 times the wall shear stress. Wind tunnel data values, in many instances, may indicate an underestimation of this ratio due to the problems experienced with low frequency effects (Willmarth²⁰). Similar low frequency problems may also be reflected in experimental results obtained with water tunnels due to the necessity of filtering out low frequencies.

Ross¹⁸ observes that for all measurements in equilibrium boundary layers, neglecting the effects of pressure gradients observed by Schloemer^{31,32} and Mugridge,⁴² the following relationship adequately describes the measured results:

$$P_{RMS} \sim 3 \cdot C_f q \sim 0.005q,$$

where

$$q = 1/2 \rho U_\infty^2.$$

Ross¹⁸ also notes that turbulent pressure fluctuations are dependent on turbulence levels that, in turn, are related to the hydrodynamic drag through the wall shear stress. This leads to the expectation that a decreasing drag would also be accompanied by a reduction in the pressure fluctuations. Furthermore, the Kraichnan estimate,¹² based on a rigid boundary and the interaction of the turbulence and mean wall shear stress, reinforces this point. (Note that many of these earlier experiments were performed without a great deal of attention to the properties of the wall and the subsequent boundary conditions on the normal pressure gradient.)

The measured ratios of the P_{RMS} to shear stress or to dynamic pressure are less than the Kraichnan value.¹² This can be explained by the relatively large diameter sensors [d/δ^+ (table 1)] used in most experiments and the high pass filtering employed to eliminate spurious low frequency noise and electrical noise.

The relationship between P_{RMS} and drag has been demonstrated by Kadykov and Lyamshev.⁴³ They confirmed that the addition of dilute polymer solutions reduces pressure fluctuations from 1 to 8 dB. This reduction in pressure fluctuation level is related to the drag reduction first reported by Toms⁴⁴ and more recently by Fabula,⁴⁵ Van Driest,⁴⁶ and many others.

NONDIMENSIONAL WALL PRESSURE SPECTRA

One of the earliest reviews on the experimental measurement of wall pressure spectra and its spatial correlation appears in the Proceedings of the Second Sym-

Table 1. A Summary of Root Mean Square Pressure Measurements

| P_{RMS}/τ_w | $P_{RMS}/q_\infty \times 10^3$ | Re_θ ($\times 10^{-3}$) | U_c/U_∞ | d/δ^* | Reference |
|------------------|--------------------------------|-------------------------------------|-------------------|-------------------|---|
| 3.2 | 9.5 | 3.8 | 0.7-0.8 | 1.2 | Harrison ¹⁹ Wind Tunnel |
| | 5.8-6.5 | 80-250 | 0.7-0.8 | | VonWinkle & Corcos ²⁸ Wind Tunnel |
| 2.4-2.5 2.64 | 5.2-5.1 5.61 | 29-38 | 0.56-0.83 | 0.33 | Willmarth & Wooldridge ²⁴ Air Tunnel |
| 1.21 (2.15-2.19) | 1.21 (4.66-4.77) | | | | Willmarth ³⁸ |
| 2.7 | 5-6 | 10-20 | 0.7-0.85 | 0.35 | Bull & Willis ³⁹ Water Tunnel |
| 2.3-2.5 | 5.5-5.7 | 13-23 | | 1.1 | Willmarth ⁴⁰ Wind Tunnel |
| 0.97 | 1.9 | 65 | 0.7-0.9 | 2.5 | Skudrzyk & Haddle ^{21,22} Water |
| | 5.4-6 | 40-160 | 0.7-0.8 | 2.5 | VonWinkle ²⁷ Air |
| | 4.0-5.6 | 100-300 | 0.65-0.95 | 0.39 | Bakewell et al. ³⁰ Water Tunnel |
| 2.66 | 5.0 | 38 | | | Willmarth & Roos ⁴¹ Air |
| 2.2-2.7 | 5.5 | 7-35 | 0.825 0.53-0.8 | 0.30 0.15-0.51 | Bull ³³ |
| 2.9-3.6 | 8.76-11.1 | 8.2-28 | 0.73-0.82 | 0.101 | Blake ³⁴ |

posium on Naval Hydrodynamics.¹⁹ During this symposium, Harrison¹⁹ presented his experimental results for a flat plate in a subsonic wind tunnel, and Skudrzyk and Haddle²¹ presented their results obtained on the surface of a rotating cylinder in the Garfield Thomas Water Tunnel. Both papers presented detailed data and clear analyses. Both experiments used sensors with a diameter-to-displacement boundary layer thickness ratio (d/δ^*) between 1.2 and 2.5. However, a large unexplained difference (factor of 5) is apparent in the two experimental determinations of the ratio of P_{RMS} to the dynamic pressure. Harrison¹⁹ observed a nondimensional spectrum with a $10 \text{ LOG } (\phi(f)/\rho^2 U_\infty^3 \delta^*) = -40 \text{ dB}$ level that was flat to a frequency $f\delta^*/U_\infty = 0.1$. Although the observed spectral level decreased rapidly, no attempt was made to compensate for transducer size. Harrison's result is consistent with the data presented in figure 1, which shows the measurements by VonWinkle²⁷ and a lower bound determined by Haddle and Skudrzyk.¹⁶ Data examined in this review lie within these limits. Also shown in figure 1 are some measurements performed on a body of revolution by Bakewell.³⁶

Possible reasons for the wide scatter in experimental results are uncontrolled experimental parameters, differences in experimental design, and transducer size. In earlier wind tunnel experiments, large low frequency energy densities ($\omega\delta^*/U_\infty < 0.1$, $f\delta^*/U_\infty < 0.016$), such as experienced by Willmarth and Wooldridge,²⁴ were encountered. Bakewell³⁶ performed measurements in water on a body of revolution for two different ranges of the ratio d/δ^* . For frequencies $f\delta^*/U_\infty < 0.1$, both sets of data are in agreement. Above this frequency, the data diverge, with that for the larger ratio d/δ^* falling off more rapidly. Application of the Corcos⁴⁷ correction was found by Bakewell³⁶ to provide excellent data coalescence for all non-dimensional frequencies, with any discrepancies being well within experimental accuracy for the measurements of both spectral level and transducer response characteristics.

Sometimes these spectra are found to peak slightly at 0.016 and decrease at the higher frequencies as much as 9 to 12 dB per octave. Bakewell's corrected spectra³⁶ decrease at 9 dB per octave for dimensionless frequencies above 1.0. The Corcos calculational technique has been confirmed by VonWinkle,²⁷ VonWinkle and Corcos,²⁸ Gilchrist and Strawderman,⁴⁸ Lyamshev and Salosina,⁴⁹ and Geib.⁵⁰

Thus, the TBL noise spectrum for a rigid boundary is fairly flat at the lower frequencies where transducer size effects may not be important. The considerable scatter in experimental results is believed to be due to uncertainties and difficulties in experimental measurement techniques. Haddle and Skudrzyk¹⁶ show that at low frequencies the spectrum is proportional to $\sim 5.7 \times 10^{-2} \rho^2 U_\infty^3 \delta$. Thus, the low frequency portion of the dimensional spectrum increases with boundary layer thickness and with flow speed.

For the higher frequency region (-9 dB/octave region), Lyamshev and Salosina⁴⁹ found that the pressure spectrum increases with the cube of the flow speed, and the spectral density increases with the sixth power of flow. Finally, a frequency is reached above which the integrated radiated noise from the boundary layer competes with pseudosonic nearfield pressure. Haddle and Skudrzyk¹⁶ present data that compare the relative importance of the radiated noise and pseudosound with the inference that the radiated noise will dominate at the higher frequencies; however, the importance of radiated noise at lower frequencies to the low wavenumber spectrum should be emphasized.

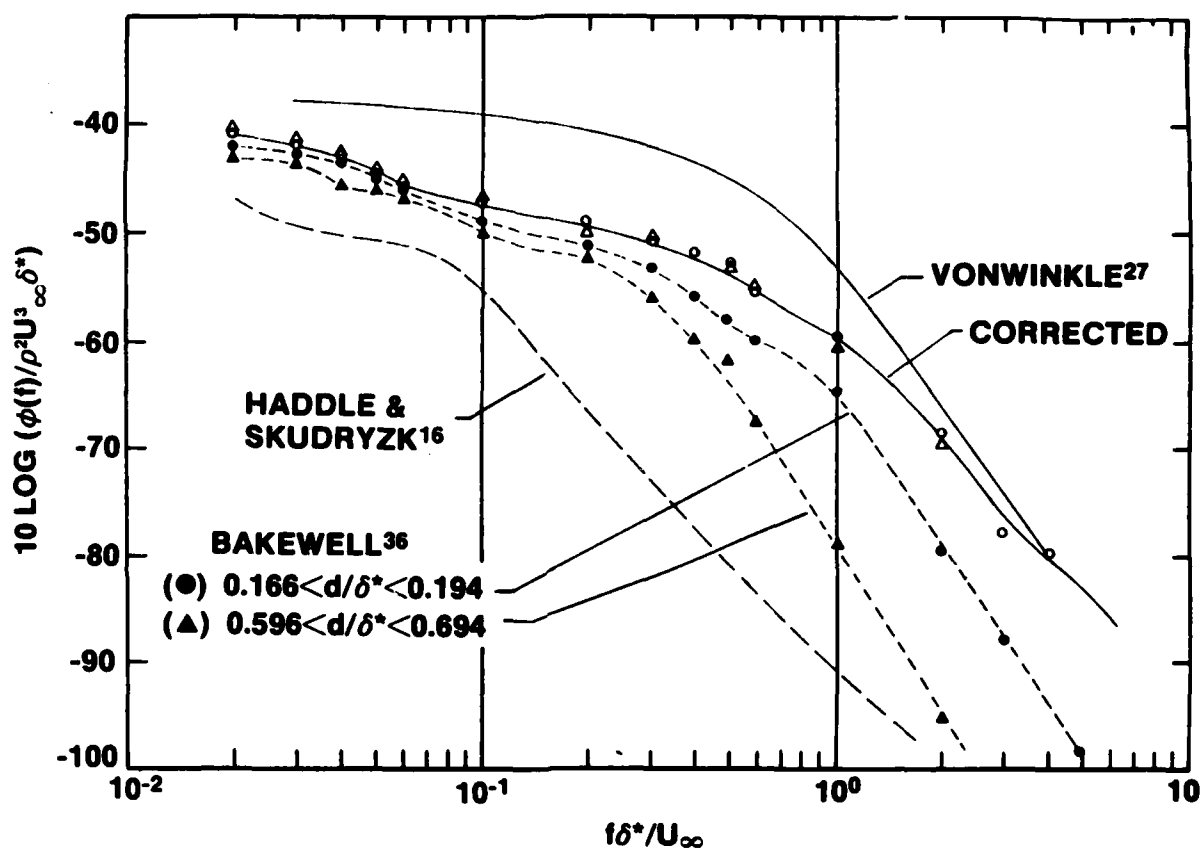


Figure 1. Dimensionless Wall Pressure Spectra As a Function of Dimensionless Frequency

CONVECTION VELOCITIES

The convection velocity associated with the lower frequency large scale turbulent eddies approaches the mean stream velocity ($\sim 0.8U_\infty$), as shown in figures 2 and 3 by Bakewell et al.³⁰ and in the earlier measurements by Harrison,¹⁹ Willmarth,⁵¹ and Von Winkle.²⁷ The scale of the eddies becomes smaller with increasing frequency and the convection velocity approaches $0.6U_\infty$ (figure 2). The convection velocity is independent of Reynolds Number (Re) for fully developed near-zero-gradient turbulent flows (figure 3). Thus, the evidence indicates that large scale turbulence originates upstream and evolves into a range of scales that are convected past the hydrophone at a velocity between $U_c \sim 0.6$ to $0.8U_\infty$. The subsequent spectrum peaks at the wavenumber $k_c = \omega/U_c$.

Recently (see Bakewell and Lumley⁵²) the role of Kline eddies^{53,54} in the generation of turbulence and flow noise has been recognized.^{16,17,34,55} Kline^{53,54} showed that turbulence is characterized by streaks of low velocity fluid that are suddenly ejected from the viscous sublayer. The significance of this periodicity is that in most of the measurements of wall pressure the sensors were too large to resolve these eddies. Haddle and Skudrzyk¹⁶ estimate that such resolution requires a 1-mm-diameter microphone for a flow of 11 m/s in air; in water, since the kinematic viscosity of water is 1/10 that of air, a 0.1-mm-diameter hydrophone is required. Both Emmerling⁵⁵ and Blake³⁴ employed pinhole techniques to measure these small scale pressure fluctuations. The dependence of measured root-mean-square (rms) pressure fluctuations on the dimensionless transducer diameter is shown in figure 4 (Emmerling⁵⁵).

Bull and Thomas⁵⁶ compared piezoelectric and pinhole microphone transducers and found that the P_{RMS} values observed by Blake³⁴ may be too large. However, the combined pinhole and optical techniques developed by Emmerling⁵⁵ and Dinkelacker et al.⁵⁷ are consistent with Blake's results.³⁴ If Emmerling's data⁵⁵ are correct, then there is evidence that the small scale wall pressure fluctuations scale with the shear velocity and wall shear stress. Secondly, the optical method discussed by Dinkelacker et al.⁵⁷ shows the progression of eddies with $U_c \sim 0.76U_\infty$ and Kline eddies^{53,54} with $U_c \sim 0.2U_\infty$. These studies suggest that a holographic examination of compliant surfaces may be a valuable tool. As Haddle and Skudrzyk¹⁶ point out, these Kline eddies, owing to their small scale and intermittent nature, can be expected to produce low frequency noise with high wavenumbers. Because of this low frequency high wavenumber effect, hydrophone size can also be important at low frequencies.

CROSS-SPECTRAL DENSITIES

Corcos⁴⁷ proposed the following functional form for the cross-spectral density of the fluctuating wall pressure:

$$\Gamma(\omega, \xi, \eta) = \phi(\omega) A(\omega \xi / U_c) B(\omega \eta / U_c) e^{-i\omega \xi / U_c},$$

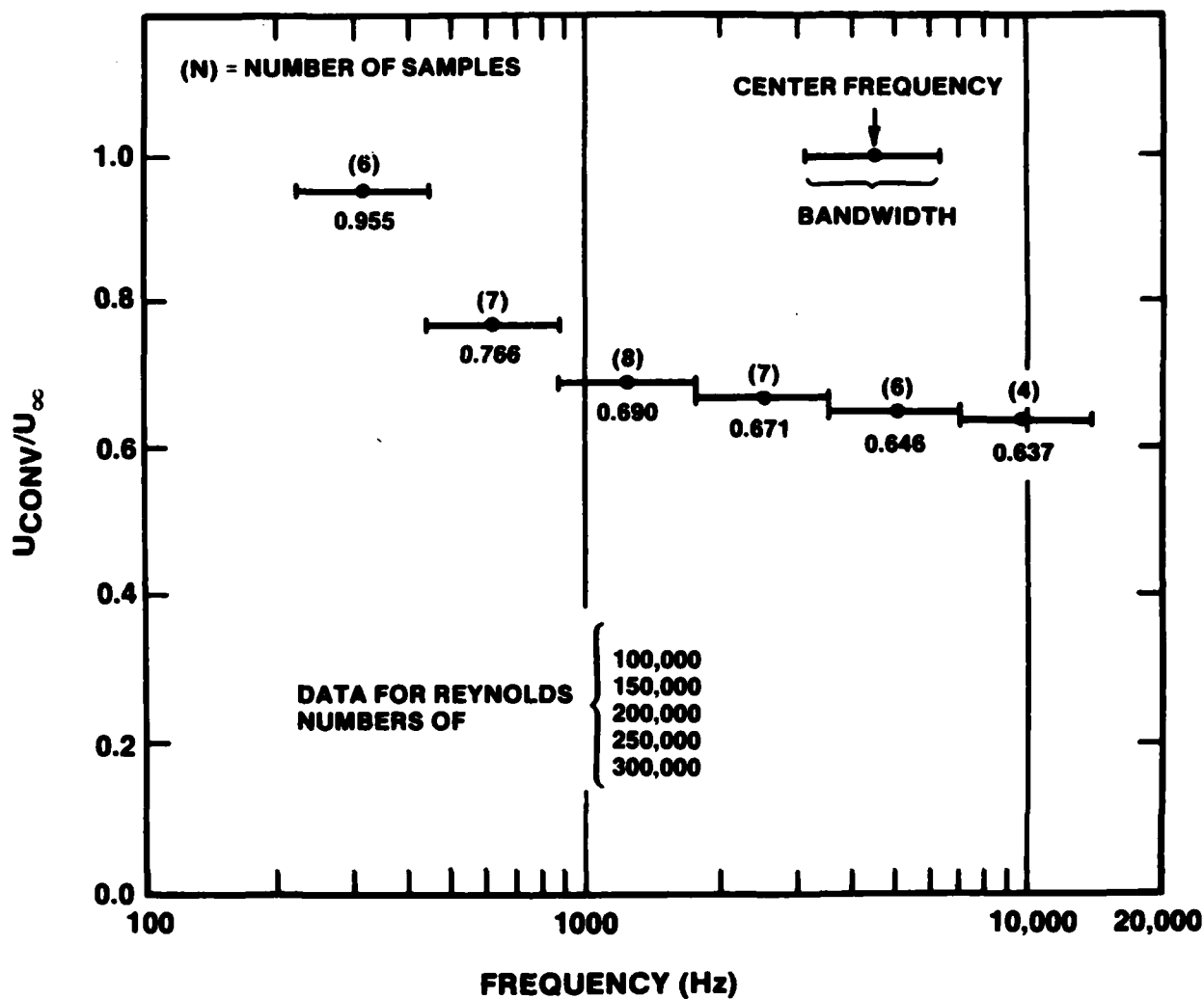


Figure 2. Ratio of Convection Velocity to Centerline Velocity
As a Function of Frequency

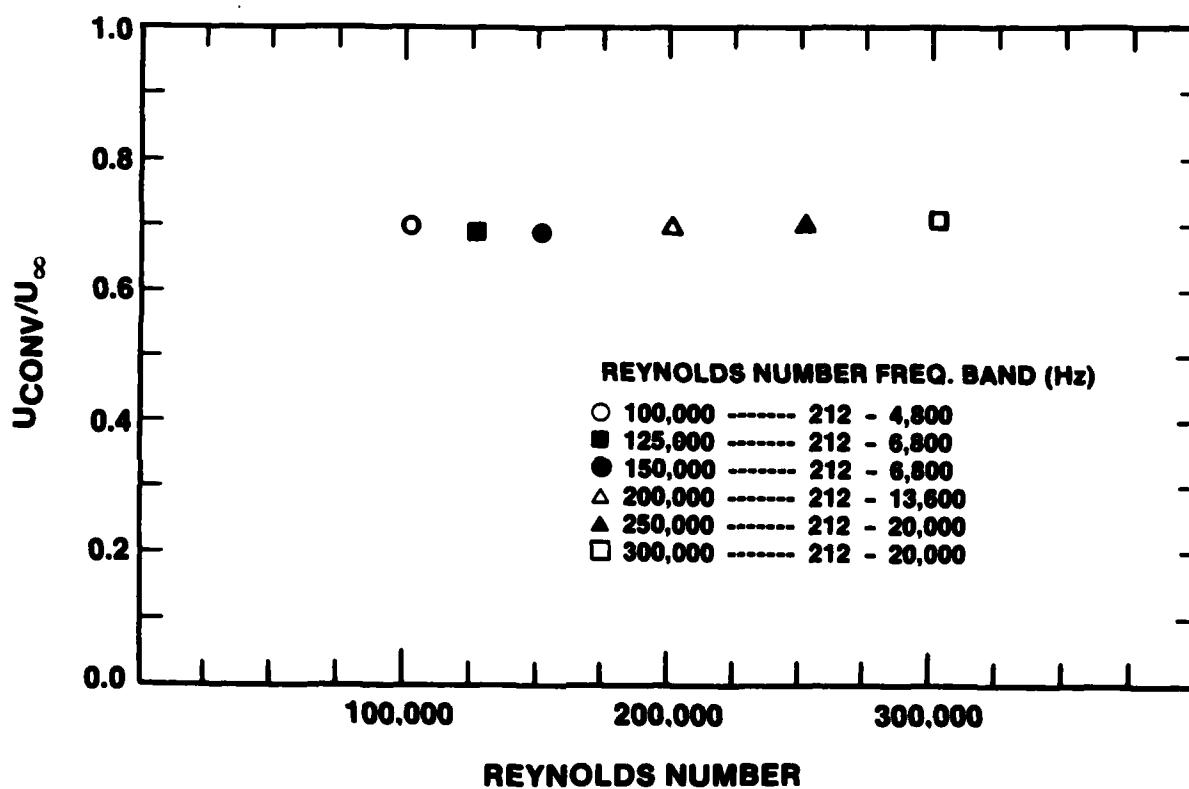


Figure 3. Ratio of Convection Velocity to Centerline Velocity
As a Function of Reynolds Number

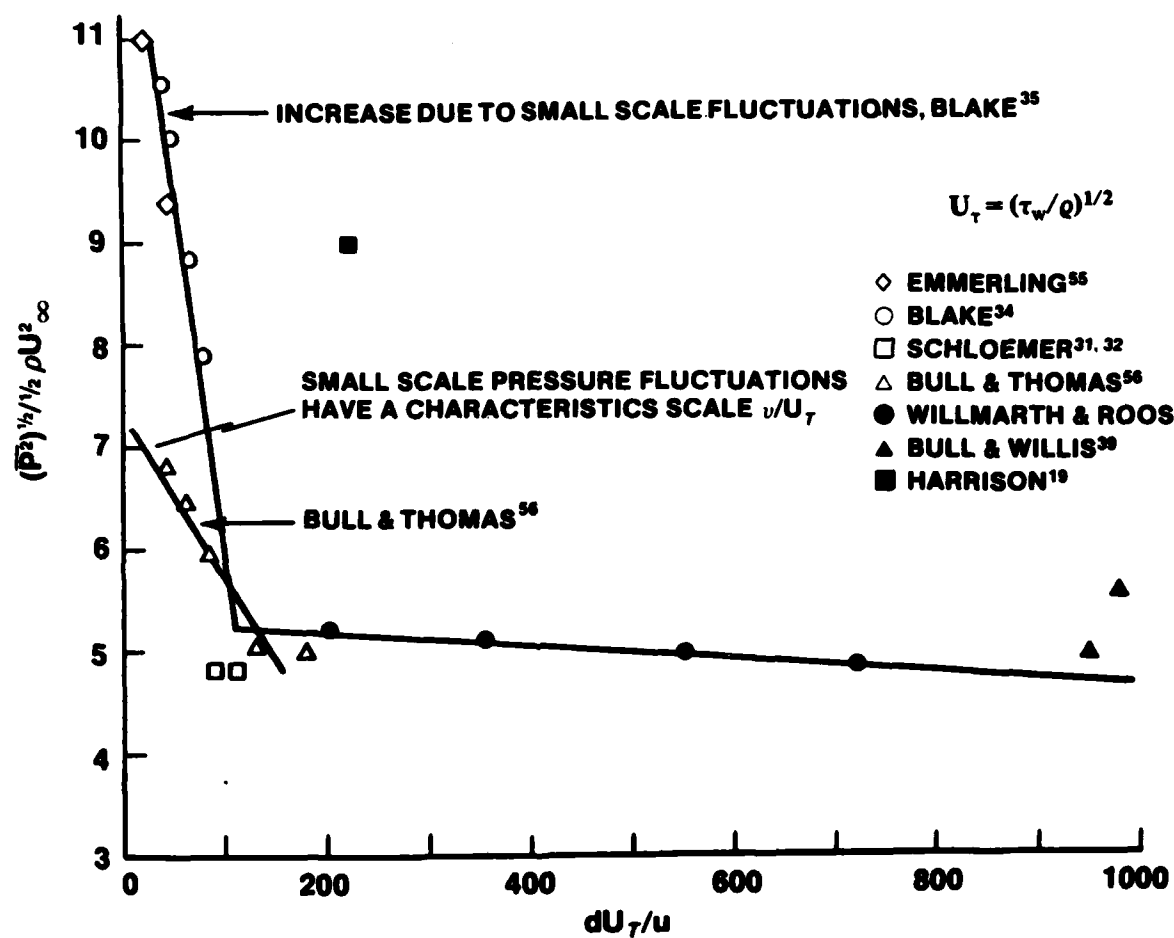


Figure 4. Dependence of Measured rms Wall Pressure Fluctuations Upon the Dimensionless Transducer Diameter

where Γ is the cross-spectral density for two sensors separated by the longitudinal distance ξ and the transverse distance η . White⁵⁸ suggested a more general form for the cross-spectral density:

$$\Gamma(\omega, \xi, \eta) = \phi(\omega) C(\omega \xi / U_c, \omega \eta / U_c) e^{-i \omega \xi / U_c}.$$

Data obtained by Bakewell³⁶ showed that the weak dependence of this C function on $\omega \delta^* / U_\infty$ can be neglected and that the separability $C \sim A \cdot B$ is valid for small separation of sensors. Measurements of this function can be obtained either from a normalized filtered correlation function or from an actual cross-spectral-density measurement. Bakewell³⁶ used the normalized filtered space-time correlation method to demonstrate the separability of the C function. His results for the longitudinal and transverse A and B functions, respectively, were in agreement with Bull²⁵ and with Willmarth and Wooldridge²⁴

Schloemer^{31,32} has also performed cross-spectral-density measurements in an acoustically quiet water tunnel utilizing a fast Fourier transform (FFT) computer routine. Figures 5 and 6 represent his results. The determination of the longitudinal A function exhibits a downturn at $(\omega \xi / U_c \sim 1.0)$, and above this value the determination agrees with Bull.²⁵ This downturn in the data is due to coherent interference of pump noise and is not a property of the flow field. Figure 6 (Schloemer³⁹) shows excellent agreement with the results of Bakewell³⁶ and Willmarth and Wooldridge²⁴ for the lateral cross-spectral density. The determination of these cross-spectral density functions is subject to the same limitation of transducer size with respect to the scales of the turbulence, as discussed earlier.

The large scale convective eddies produce a rather complex picture from a statistical viewpoint. Figure 7 shows the wall pressure cross-correlation coefficient as a function of time delay and longitudinal sensor separation as measured by Willmarth and Wooldridge.²⁴ The Corcos cross-power spectral density functions⁴⁷ show the lateral and longitudinal coherent decay of the turbulent eddies. These functions have been useful in compensating for finite transducer cancellation effects. This plot of the correlation coefficient shows a ridge of large pressure correlations extending into the first quadrant and decaying in amplitude. Willmarth and Wooldridge²⁴ explain this ridge as due to the downstream convection of pressure-producing eddies that lose their "identity" (coherence) with distance.

The trace of this correlative peak is not projected as a straight line in the x_1 / δ^* , $\tau U_\infty / \delta^*$ plane, but as a curved line. As the distance from the origin increases, the slope of the projected ridge in the x, τ plane increases. The slope of this projected line can be considered as the convection velocity; for small sensor separation, this velocity is smaller than for large separations, x_1 . Physically this indicates that the small scale turbulence becomes incoherent in a shorter spatial time than does the larger scale turbulence. Willmarth and Wooldridge²⁴ further mention that large scale disturbances extend farther from the wall where the mean velocity is greater; and, consequently, these large scale eddies retain their coherence over longer distances. This effect could be related to the Kline eddies^{53,54} and measurements by Emmerling.⁵⁴

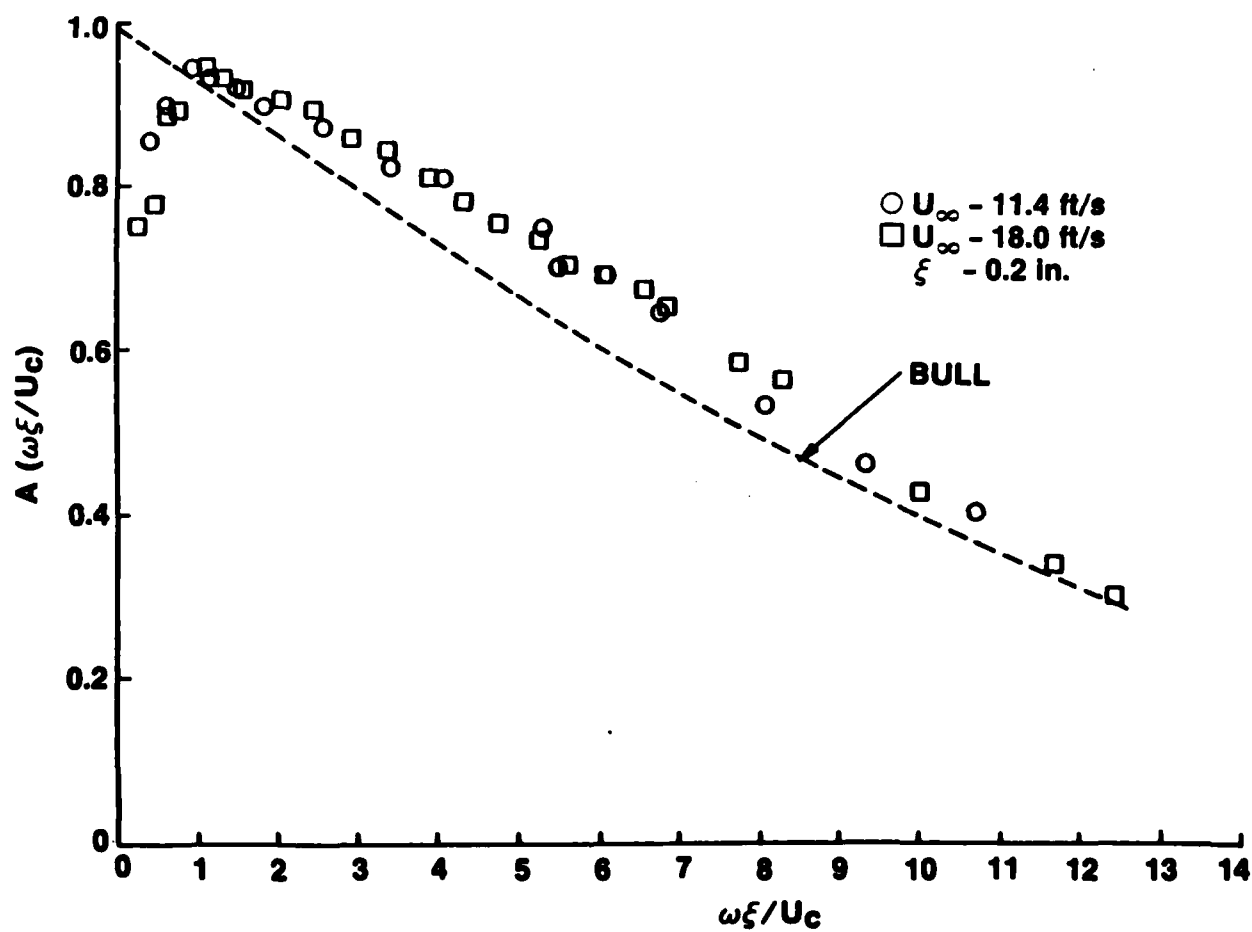


Figure 5. Magnitude of the Normalized Longitudinal Cross-Spectral Density

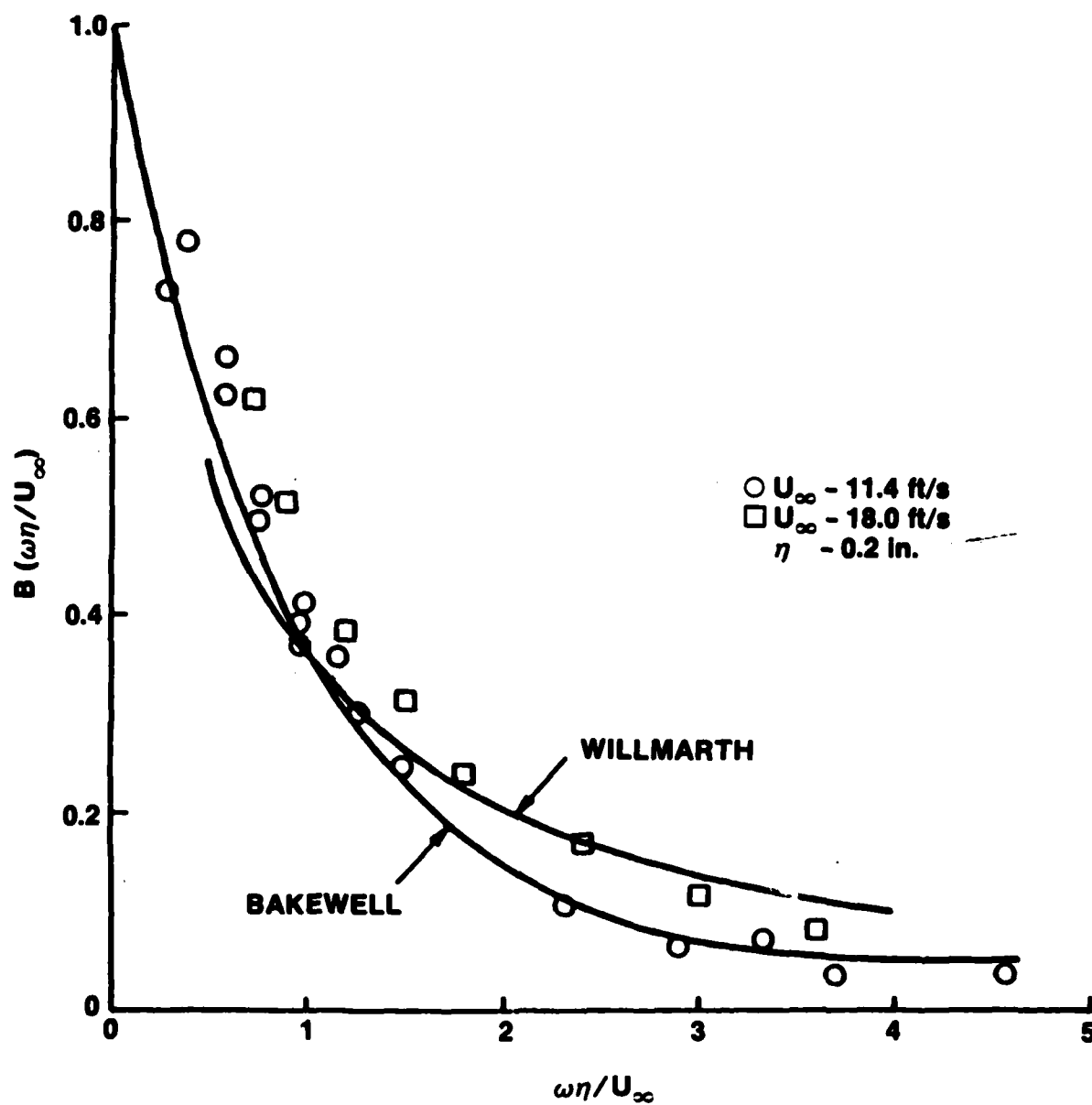
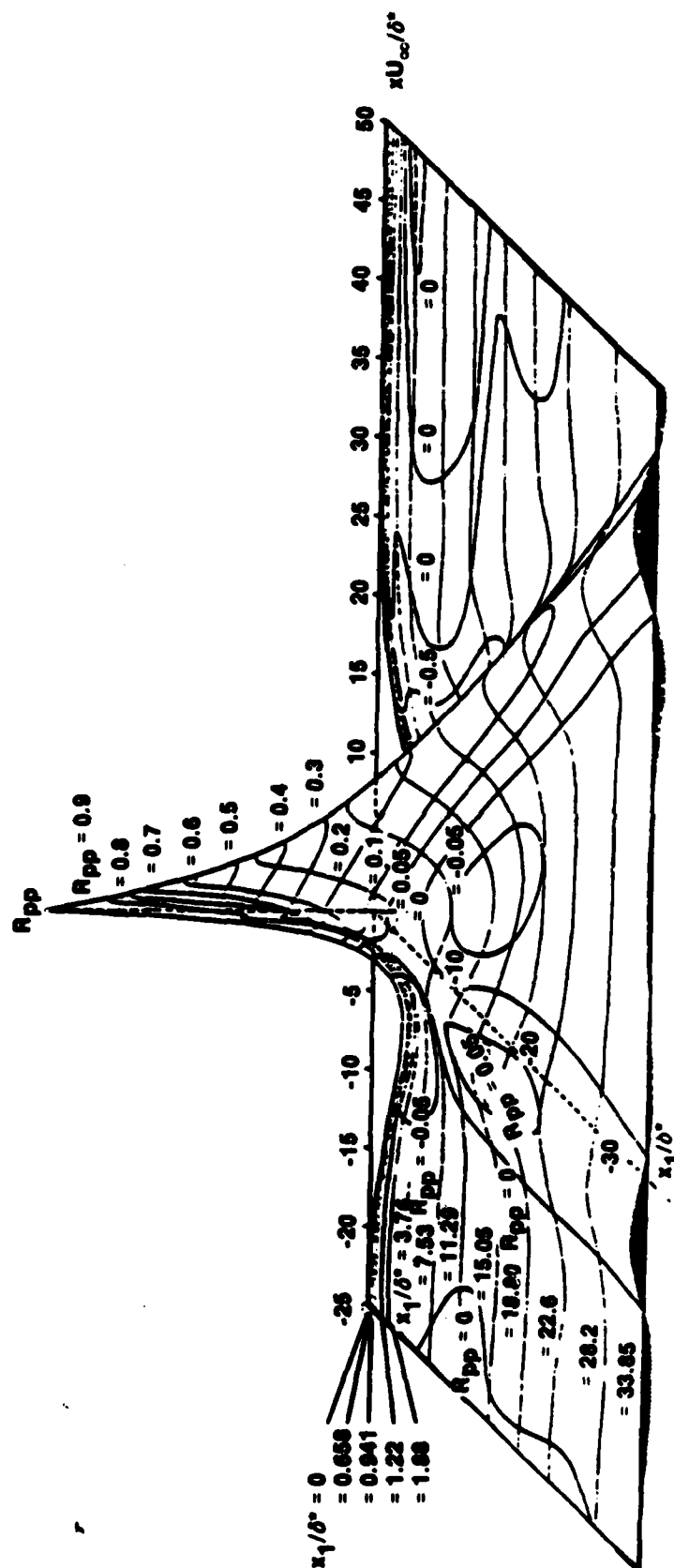


Figure 6. Magnitude of the Normalized Lateral Cross-Spectral Density



NOTE: CONTOUR LINES ARE THOSE OF CONSTANT CORRELATION R_{pp} .

Figure 7. Longitudinal Space-Time Correlation of the Wall Pressure As a Function of Nondimensional Transducer Separation, x_1/δ^* , and Time Delay, $\tau U_\infty/\delta^*$

An alternative method of viewing this convective energy is to consider the wavenumber spectrum. The cross-spectral density is defined as

$$\Gamma(\omega, \underline{x}) \equiv \frac{1}{\sqrt{2\pi}} \int_{-\infty}^{\infty} dt \cdot R_{pp}(\underline{x}, t) e^{-i\omega t}.$$

The spectral density of this cross-spectral density, $\Gamma(\omega, \underline{k})$, is

$$\Gamma(\omega, \underline{k}) \equiv \frac{1}{\sqrt{2\pi}} \int_{-\infty}^{\infty} d\underline{x} \Gamma(\omega, \underline{x}) e^{-i\underline{k} \cdot \underline{x}},$$

where ω is the Fourier conjugate of the temporal variable t , and \underline{k} is the Fourier conjugate of the spatial vector variable \underline{x} . A representative wavenumber spectrum at constant frequency (ω) is shown in figure 8 (Haddle and Skudrzyk¹⁶) illustrating the sharp convective peak at wavenumber $k = \omega/U_c$, where U_c is the convective velocity. Haddle and Skudrzyk¹⁶ estimate that the decay lifetime of a large scale turbulent eddy is $30\delta/U_c$, which is of the order of $1/30$ s. This corresponds to a $\Delta f \sim 30$ and a $\Delta k = \Delta\omega/U_c = 2\pi(30)/U_c \sim 200/U_c$, as shown in the figure. For a freestream velocity $U_\infty = 11$ m/s and a frequency of $f = 100$ Hz, the wavenumber of the convective peak ω/U_c is approximately 95.2 m^{-1} , whereas the wavenumber for acoustic propagation is 0.41 m^{-1} . In principle the wavenumber spectrum provides separation of radiated noise from convective TBL noise and, consequently, of the spectral levels of the convective peak, $P(k_c, \omega)$, and the radiated noise peak, $P(k \ll k_o, \omega)$. Although such measurements are generally not simple, an example of the relative contributions of radiated and convective energy is provided by Haddle and Skudrzyk's¹⁶ measurements at 42 knots on a body of revolution. These measurements show that at 300 Hz the radiated noise level at the surface was 30 to 40 dB lower than the wall pressure fluctuation, whereas the two contributions became equal at 1 kHz. (Note that bursts or Kline eddies^{53,54} for the case discussed above are located far to the right of k_c at wavenumber $k_k \sim 628/(0.2) \cdot (11) = 285 \text{ m}^{-1}$ in figure 8.)

This concludes the brief overview of the spectral and cross-spectral properties of TBL noise in flows on rigid surfaces that do not interact with the flow. The discussion, while largely qualitative, has been based on the extensive body of experimental evidence available and further suggests that additional analytical and experimental clarifications are necessary.

COMPLIANT SURFACE EXPERIMENTS

Several compliant-surface experiments have been performed as a result of the work of Kramer² and Boggs and Tokita⁶⁰ who were intrigued with the possible role that the skin of the porpoises and whales has on the drag experienced by these mammals. On the premise that reduction in drag could mean a reduction in noise,

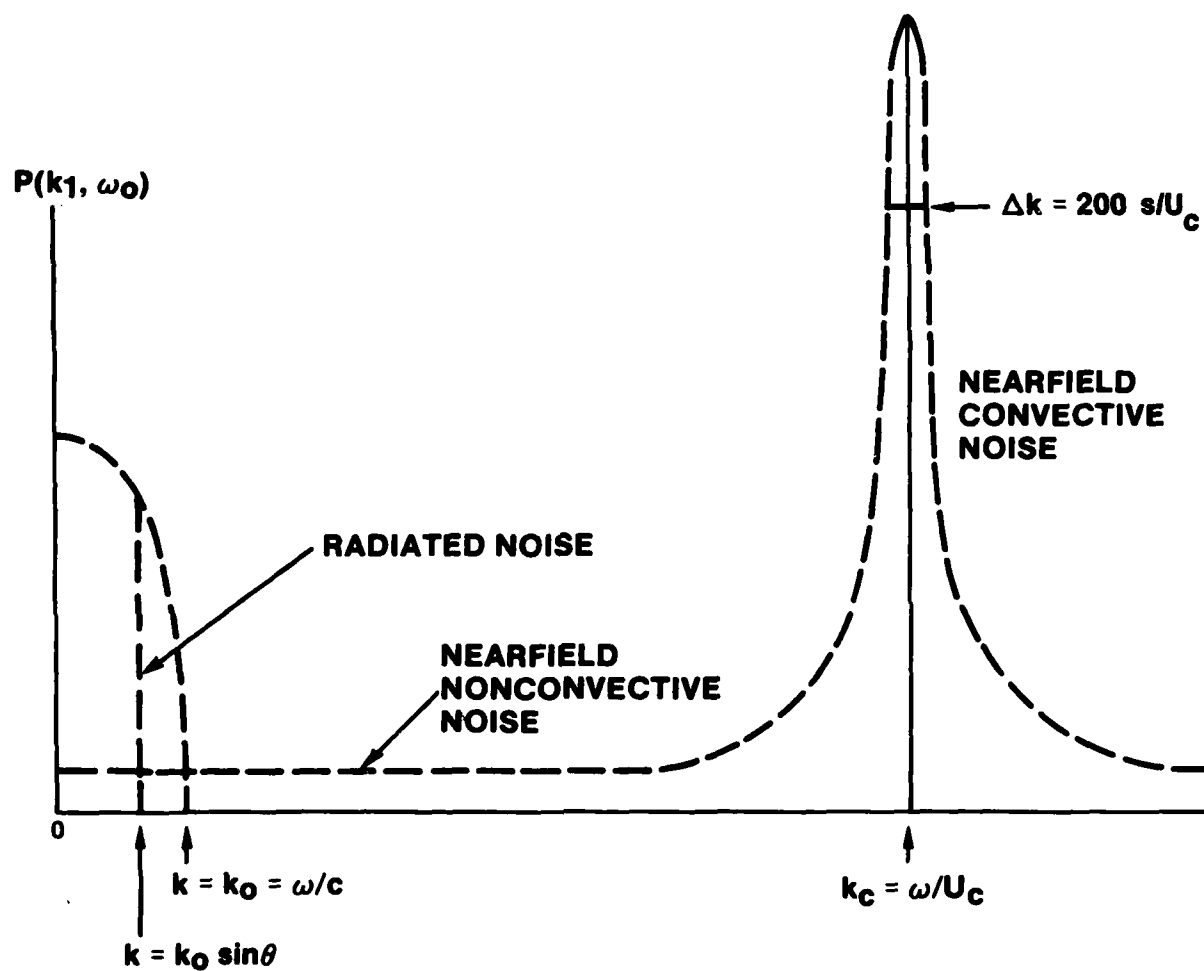


Figure 8. Typical Longitudinal Wavenumber Spectrum for Constant Frequency ω_0 Showing Location of Nearfield and Radiated Noise Components

with a compliant surface on top of a rigid surface influencing the characteristics of the TBL, VonWinkle³⁵ and VonWinkle and Barger⁶¹ continued this work with a material known as LAMIFLO,* "porpoise skin" coating. They observed that the boundary layer was affected, that the pressure coefficient was an order of magnitude lower, and that with the coating in place the overall power spectra of the pressure fluctuations were reduced over a wide range of frequencies. The maximum reductions were of the order of 25 dB. This work was followed by a Naval Underwater Systems Center (NUSC) study conducted by G. Carey et al.³⁷ This study concluded that within a 95-percent confidence limit the data showed the compliant coatings to cause a frequency-dependent effect on the TBL noise. Noise reductions ranged from only 4 to 13 dB. These experiments, conducted in a facility subject to significant changes in water temperature, further provided definite evidence of the importance of temperature on the effectiveness of the coatings.

The Soviets, particularly Babenko⁶² and Babenko and Surkina,⁶³ have performed exhaustive tests on dolphins to characterize their skins and the effects of compliance on flow stability. This remarkable work can be summarized by noting that rather complex sets of effects, not easily explained, were observed in the flow noise experiments, flow stability experiments, and stability calculations.

Despite the exhaustive experiments conducted with compliant materials for both drag and noise reduction, no single investigation has yet adequately described the material properties as a function of frequency and temperature.

Figure 9 shows the experimental setup and test body schematic for VonWinkle and Barger's⁶¹ experiments that were conducted in a constant temperature facility with a temperature-stabilized vehicle. The coated test body had a LAMIFLO covering constructed from a soft natural rubber with support pedestals. The intervening volume between the pedestals was alternately filled with air, water, and other fluids of different viscosities up to 1000 centistokes for different data runs. Monitor hydrophones fabricated from commercially available lead-zirconate titanite were flush mounted with the surfaces of the coated and control test bodies. The velocity time history of the test body was recorded during each free-fall of the test vehicle, and the corresponding power spectra were obtained with a 1/3-octave analyzer. Figure 10 shows the rms sound pressure level (SPL) as a function of velocity obtained from hydrophone no. 2 for the control and coated body with two different fluids. The reference line shows the relationship of rms pressure and velocity for a pressure coefficient of 0.006, which is representative of fully developed turbulent flow. These data indicate that, for the control body and the LAMIFLO coating with air, the pressure coefficients are 0.0047 and 0.0054, respectively, which are comparable to the reference case (0.006). The water-filled LAMIFLO coating resulted in an order of magnitude reduction in the pressure coefficient to a value of 0.00054. It can be seen that the pressures for both the control body and the body with an air-filled coating are similar and close to those representative of a fully developed TBL. The data for the case of the water-filled coating, however, indicate that pressures representative of a normal TBL are never reached over the test velocity range. Whether this is at least in part a result of a downstream shift or delay in transition is not known.

In figure 11 the frequency spectra of the wall pressure fluctuations obtained with the hydrophone at location no. 2 are shown for the uncoated body and both the

*U.S. Rubber Co. trademark.

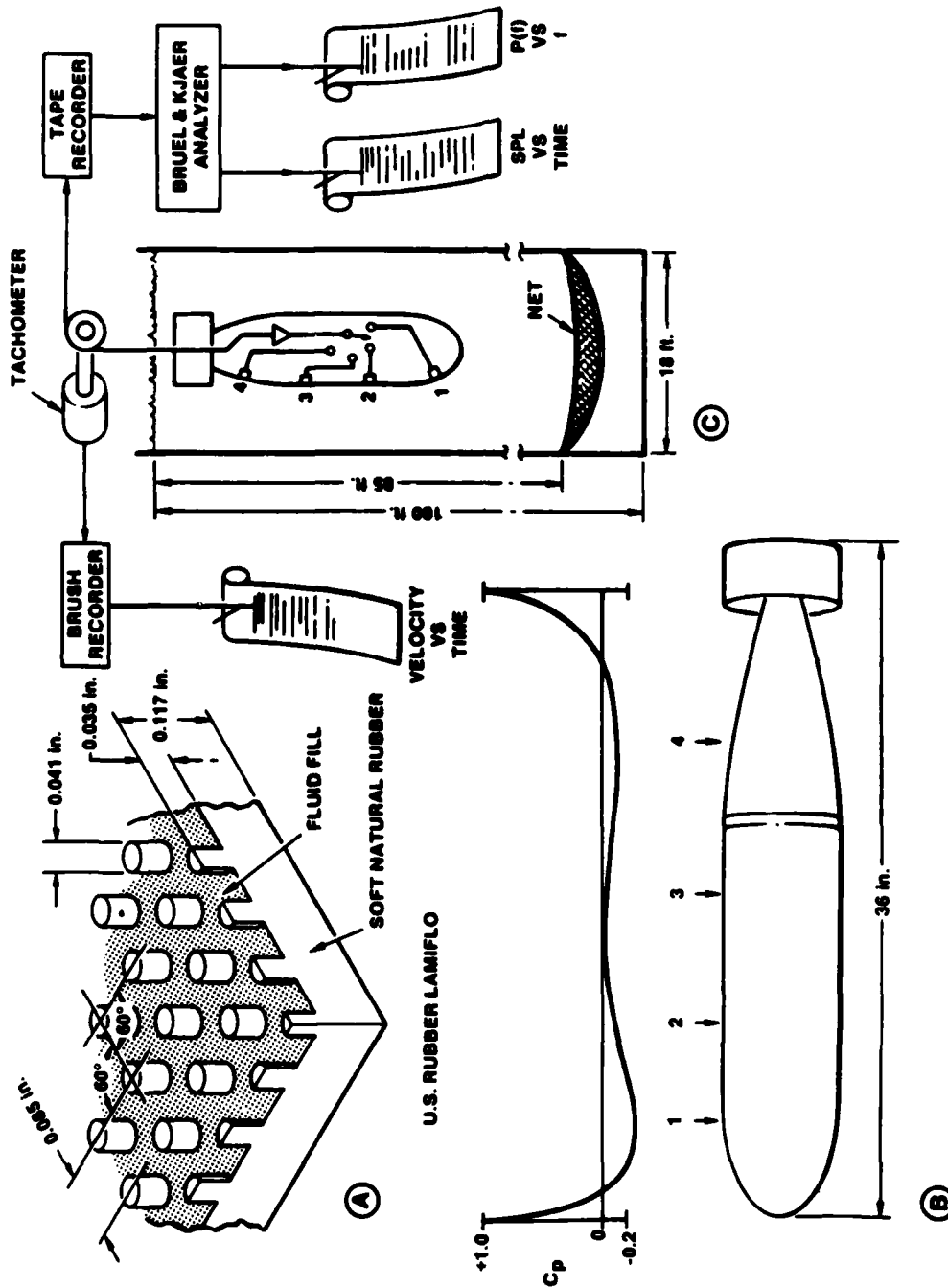


Figure 9. Noise Investigations

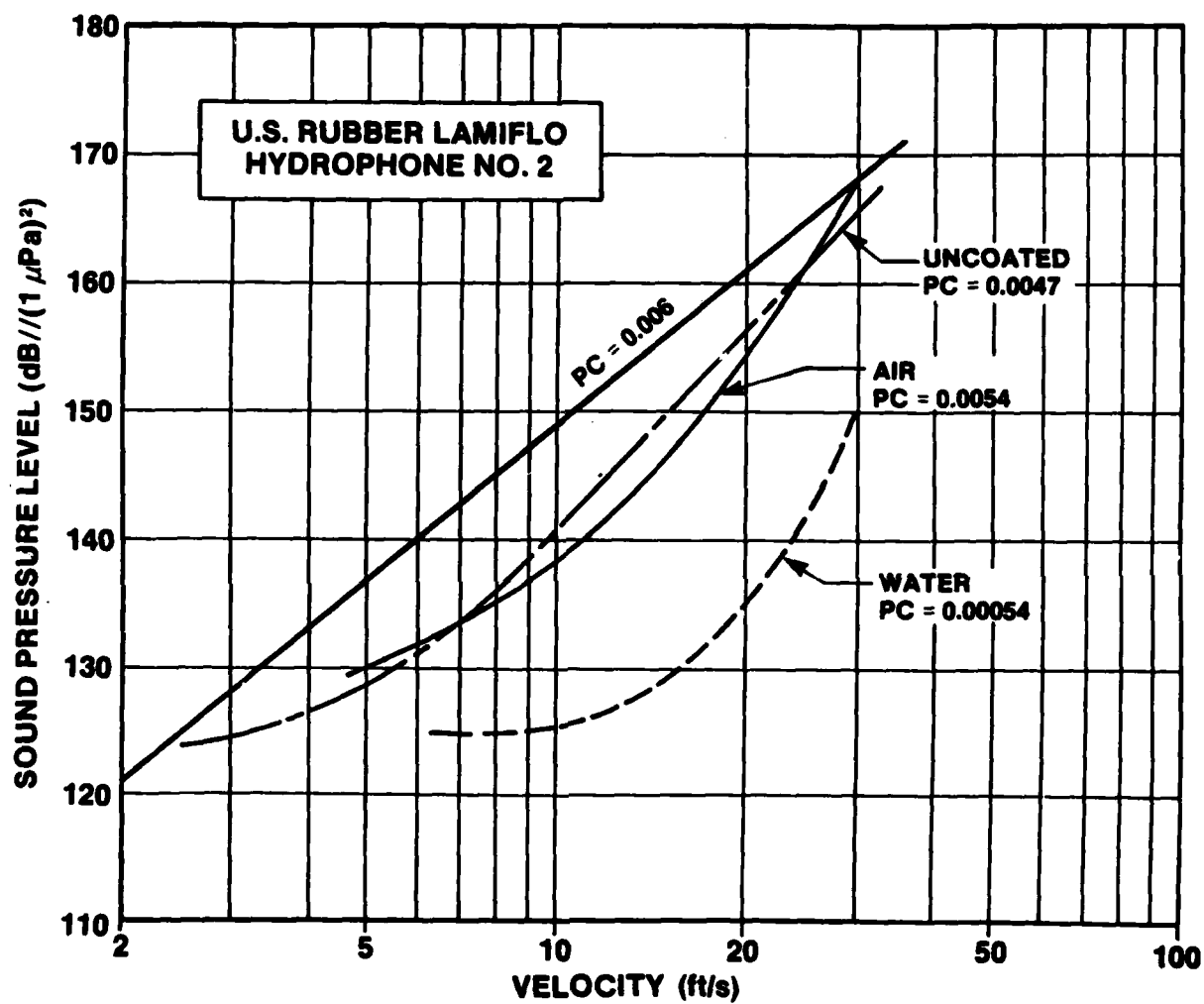


Figure 10. Broadband Sound Pressure Level As a Function of Vehicle Velocity Measured With Hydrophone No. 2

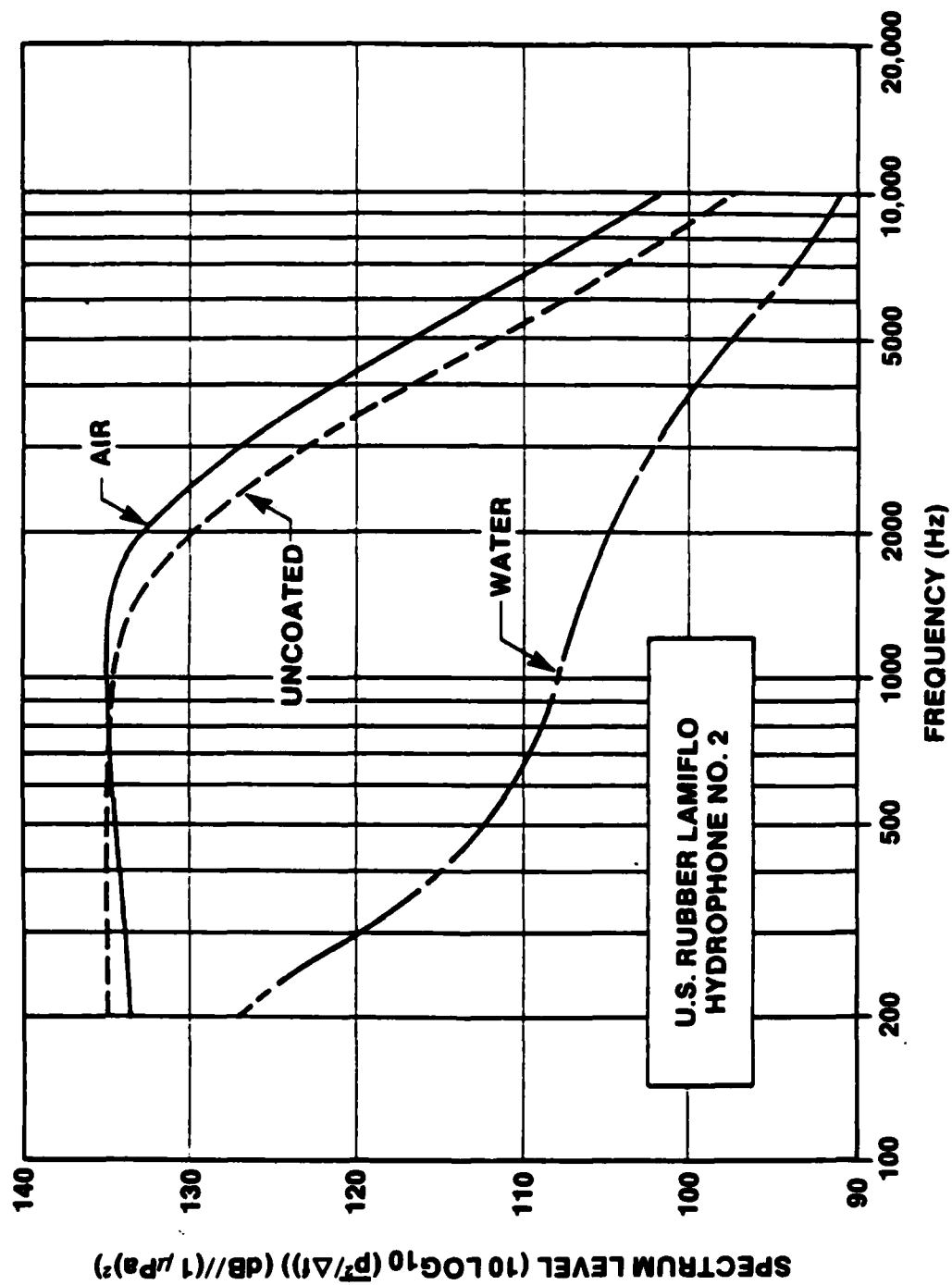


Figure 11. Dimensional Wall Pressure Spectrum As a Function of Frequency Measured With Hydrophone No. 2

water- and air-filled coatings. The difference in pressure coefficients for these three cases was noted in figure 10. These coefficients were computed at the terminal velocity of the body. The power spectrum for the uncoated control body with a pressure coefficient of 0.0058 in figure 11 exhibits a general shape representative of power spectra measured by Willmarth,²⁰ Harrison,¹⁹ and others¹⁶ for the TBL. The spectrum for the water-filled LAMIFLO coating exhibits a distinctly different shape, as well as markedly lower levels of wall pressure fluctuations. The maximum pressure reduction occurs near 1 kHz. (It is interesting to note that the wavelength in a pressure pattern passing the hydrophone at the terminal velocity that corresponds to this frequency is about equal to the wavelength of unstable pressures, as predicted by the Schlichting stability theory.) Although tests were conducted with fluids of other viscosity within the coating, no noise reductions greater than those shown in figure 11 for the water-filled coating were obtained.

An experiment utilizing a free-falling streamlined body of revolution was conducted by Carey et al.³⁷ to evaluate the effects of three compliant coatings on TBL wall pressure fluctuations. Data obtained from the coated vehicles showed considerably more variation in rms pressure levels than that for the uncoated control or reference vehicle. This variation, which could not be explained by experimental errors alone, necessitated a statistical treatment of the data. Within a 95-percent confidence limit, the data indicated that the compliant coatings did result in a frequency-dependent change in the TBL wall pressure fluctuations. On one occasion, the maximum noise reduction reached 13 dB, but the 95-percent confidence interval between coated and uncoated cases never separated by more than 4 dB in the frequency band from 2 to 5 kHz. These data on different coatings further illustrated a complex temperature dependence evidenced by an average decrease in the rms pressure level of 0.5 dB per degree Fahrenheit temperature increase within the temperature range of 39° to 69° F. This temperature dependence of the measured wall pressure fluctuations is believed to be attributable to the temperature-dependent moduli of the coating.

In summary, reductions in the measured flow noise on a compliant surface have been observed for both the LAMIFLO material and other solid coatings. The measured pressure coefficients noted were as much as an order of magnitude lower than those observed in a fully developed turbulent flow on uncoated control bodies. The reductions in noise were not, however, systematic and further exhibited a complex temperature dependence that was not fully characterized. Nevertheless, the power spectra of the wall pressure fluctuations with coatings in place were found to be reduced to a varying degree over a relatively wide band of frequencies.

PRELIMINARY MATERIAL MEASUREMENT

The TBL wall pressure fluctuations have been discussed in terms of both spectra and spatial correlative properties. An example of the TBL wall pressure spectrum is shown in figure 11 to extend over a range of frequencies up to 10 kHz. It is precisely over this same frequency range that the properties of compliant materials should be characterized for definitive determination of their effect on the TBL. The basic criterion for the characterization of a viscoelastic material is the knowledge of 36 viscoelastic coefficients. For isotropic materials, 24 become zero

and the remainder are expressed in terms of two basic constants, the Lamé's constants. These two constants, in turn, can be described by any two of the three standard moduli: The Bulk, Shear, and Young's Moduli. For rubberlike materials, where Poisson's ratio approaches 0.5, only one modulus is required to characterize the material, and the experimental determination of the complex Young's or Shear modulus as a function of frequency and temperature will meet the need for complaint surface studies. Several reviews on the dynamic measurement of viscoelastic properties, such as those by Cramer,⁶⁴ Solarek,⁶⁵ and Carey, Doolittle, et al.,⁶⁶ are available and, hence, will not be discussed in this document.

An extensively used technique for measuring the complex dynamical mechanical Shear modulus is the Fitzgerald apparatus introduced by Fitzgerald and Ferry⁶⁷ at the University of Wisconsin in 1953. The instrument is capable of absolute calibration and yields measurement with an accuracy of ± 2 percent. The apparatus is versatile, and has been widely used by Professor Fitzgerald and many others. Its operating frequency is given as 10 to 5000 Hz, and sample temperature control is possible over a wide range of temperatures. Samples of materials from a soft gel to a hard glassy solid with dimensions of up to 1/4 in. thick and 1 in. in diameter can be tested. Typically strains from 10^{-3} to 10^{-6} are employed.

Before the characterization of dolphin's blubber, several other compliant materials had been characterized, using this Fitzgerald apparatus, to determine the complex shear compliance (defined as the reciprocal complex Shear modulus ($J^* = J' - iJ'' = 1/G^*$)) and loss tangent shown, respectively, in figures 12 and 13. The complex shear compliance of pork-belly fat (PBF) was measured at room temperature over a frequency range of 50 to 2500 Hz. The average "dead time" of the specimen was 3 hours. Results obtained with this material are compared to those for honey (HON), natural rubber stock (NRS), polyvinylchloride (PVC), polyurethane rubber (PUR), and beef-belly fat (BBF) in figures 12 and 13. At 100 Hz the PBF is approximately 1500 times as compliant as BBF or, alternately, the BBF is 1500 times stiffer than PBF. Since the pig's teats are distributed along the belly, the fat samples may be representative of the mammary gland fat. It is currently expected that the BBF properties more closely resemble the properties of dolphin's blubber than the PBF properties.

Referring to figure 12, the elastic compliance component, J' , for PBF has a value of $\sim 32.0 \times 10^{-6}$ cm²/dyne at 50 Hz, a value of $\sim 27.5 \times 10^{-6}$ cm²/dyne at 100 Hz, and has decreased to $\sim 11.0 \times 10^{-6}$ cm²/dyne at 500 Hz. By contrast, the loss of the viscous compliance component, J'' , starts from a value of $\sim 6 \times 10^{-6}$ cm²/dyne at 50 Hz, increases to a peak value of $\sim 15 \times 10^{-6}$ cm²/dyne at 150 Hz, and then decreases to a value of $\sim 6 \times 10^{-6}$ cm²/dyne at 500 Hz, which is representative of a relaxation.

Note that the general shapes of the compliance curves as functions of frequency for both the PBF and the BBF are substantially the same except for the frequency displacement; i.e., J'' (PBF) shows a peak at ~ 250 Hz and J'' (BBF) shows a peak at ~ 2500 Hz. The shapes of these curves imply relaxation dispersions in the vicinities of the peak frequencies.

Further examination of the results for the two fats in figure 13 shows that the shear loss tangent, $\tan \delta = J''/J'$, for PBF has a value of ~ 0.20 at 50 Hz and

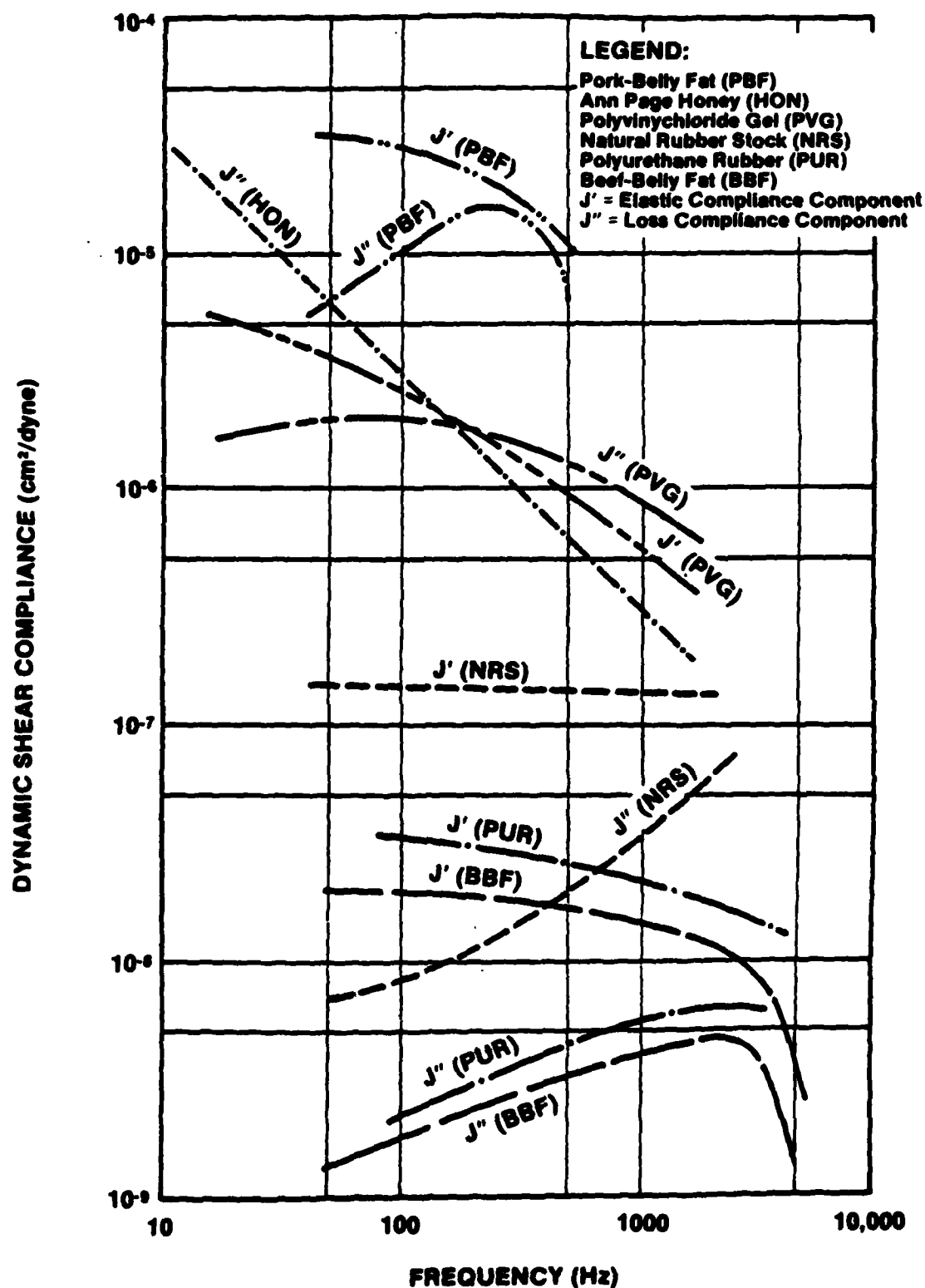


Figure 12. Complex Shear Compliance As a Function of Frequency for Selected Materials

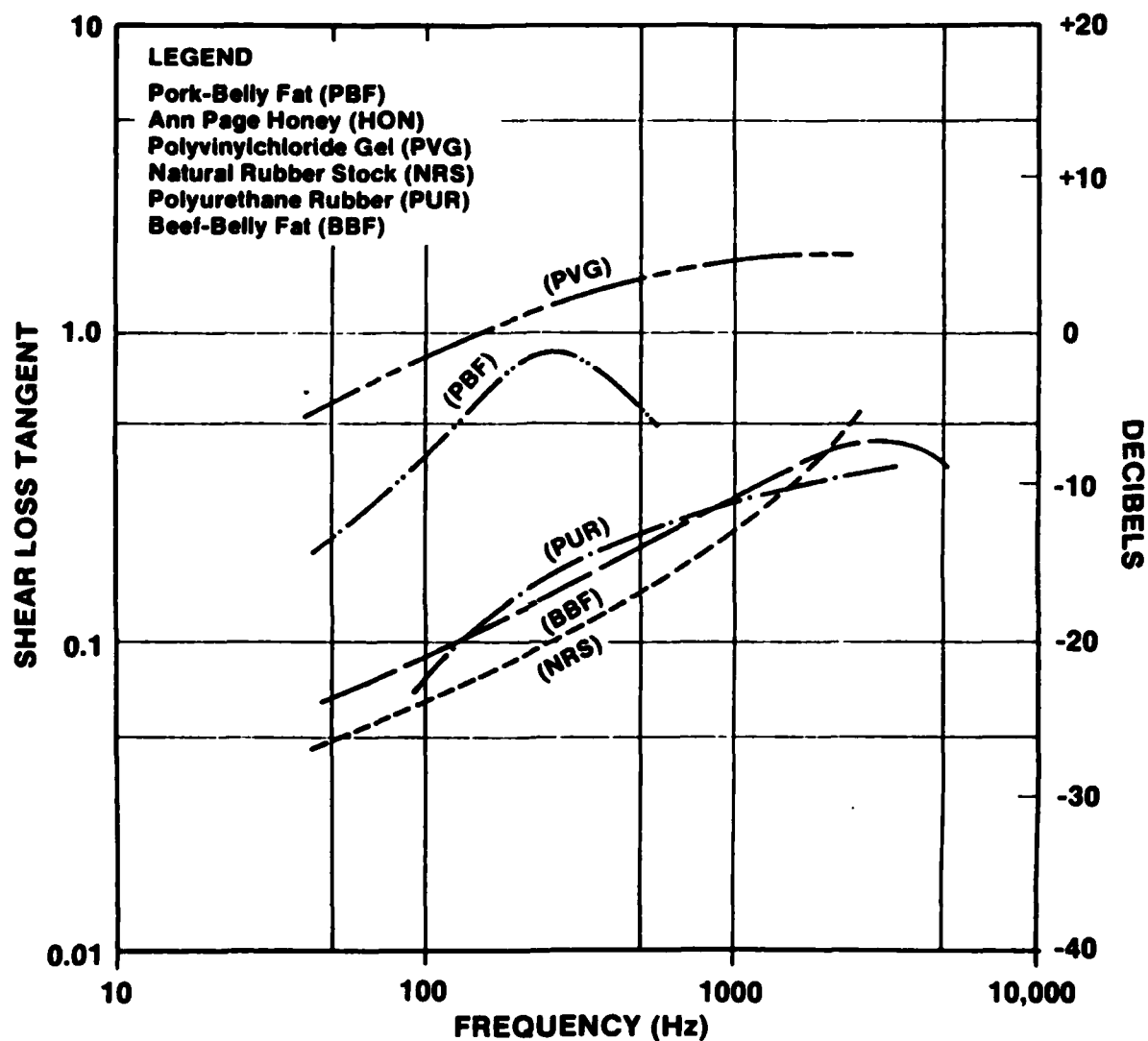


Figure 13. Shear Loss Tangent As a Function of Frequency for Selected Materials

~ 0.85 at 250 Hz. At higher frequencies, the loss tangent decreases, reaching a value of ~ 0.55 at 500 Hz. The loss tangent curve for BBF has the same general shape as that for PBF, although the peak occurs at the higher frequency of ~ 300 Hz and as a lower value of ~ 0.45 . Compared to PBF results, the relaxation peak appears to be somewhat broader for BBF. Throughout the frequency range of 50 to 500 Hz, the loss tangent (which is equal to the reciprocal of the mechanical Q) of PBF is at least 10 dB higher than that for BBF.

As shown in figures 12 and 13, PUR has complex compliance with loss tangent values that are reasonably close to those of BBF throughout the frequency ranges. However, the complex compliance of a lightly vulcanized NRS is considerably different from that for either of the fats, as can be seen in figure 12. The J' for NRS is nearly independent of frequency, with a value of $\sim 1.5 \times 10^{-7}$ cm²/dyne that is intermediate between the values for the two fats. The J'' increases, more-or-less uniformly, from a value of $\sim 8 \times 10^{-9}$ cm²/dyne at 100 Hz to $\sim 7 \times 10^{-8}$ cm²/dyne at 2500 Hz.

Throughout the frequency range of 50 to about 2000 Hz, the loss tangent for NRS, as shown in figure 13, is somewhat lower than those for both BBF and PUR, and then becomes slightly larger at higher frequencies reaching a value of ~ 0.5 at 5000 Hz.

Another material of interest shown in figure 12 is a polyvinylchloride (10%) dimethylthianthrene (90%) gel (PVG). It has a complex compliance that is much higher than the BBF, but still only about 1/10 that of PBF. The loss tangent, shown in figure 13, for PVG, however, is exceptionally high, being over 1.0 for much of the frequency range and reaching a value of nearly 2.0 at 2500 Hz.

Finally, for comparison, the loss compliance, J'' , for HON is also shown as a function of frequency. It will be recalled that the complex viscosity is defined by

$$\eta^* = \eta' - i\eta''$$

and

$$J^* = -i \left(\frac{1}{\omega \eta^*} \right).$$

In this case, HON is a classic Newtonian viscous liquid with essentially no elastic component ($J' = \infty$, or $G' = 0$). It can be seen that at ~ 100 Hz the J'' for both HON and PBF are equal, but at higher frequencies PBF is considerably more compliant ($\sim 10 \times$) than even HON!

In summary, complex shear compliance data have been obtained with the Fitzgerald apparatus on materials spanning 5 orders of magnitude. Materials from HON to PBF have been characterized as a precursor to the measurement of the properties of dolphin's blubber. The measurements performed on two mammalian tissues, BBF and PBF, show a characteristic frequency-dependent loss tangent curve. The PBF is ~ 1500 times more compliant, and the characteristic loss tangent relaxation peak value of 0.85 occurs at a frequency of 250 as compared to the BBF peak value of 0.45, which occurs at a frequency of 3000 Hz. Thus, the use of the

Fitzgerald apparatus in determining the complex properties of live mammalian tissues has been demonstrated. The next logical step is the application of this technique to determine the properties of dolphin's blubber.

PROPOSED EXPERIMENT

Central to the theme of this document is the question "What role does surface compliance play in reducing drag, hydrodynamic noise, and radiated noise?" This is not a simple question to answer and this document has attempted to highlight the need for an interdisciplinary approach to the problem. Although the experimental compliant surface investigations discussed in this review are noteworthy, the material selections were intuitive and the material properties of the surfaces were not characterized. The irreproducibility of the experimental results attest to this fact. With the proper material selection and characterization, the results can be clarified.

MATERIAL MEASUREMENT REQUIREMENTS

The characterization of the dynamic mechanical properties requires a knowledge of the temperature-frequency dependent complex shear moduli. Also, the measurement of the properties of dolphin's blubber necessitates consideration of the dead time of the blubber. With the Fitzgerald apparatus the complex shear compliance of the dolphin's blubber should be determined over the frequency range of 10 to 5000 Hz and over a temperature range of 0° to 30°C. These mechanical properties of the dolphin's blubber need to be interpreted and characterized as a function of time after removal (from the dolphin) and extrapolated to zero dead time. The sound velocity, density, and the acoustic impedance should be measured over the 0° to 30° C temperature range. The determination of the dynamic properties of dolphin's blubber will form a baseline set of parameters for the comparison, selection, and synthesis of compliant materials for use in TBL studies. Use of shear compliance values of 1/2, 1, and 2 times the measured value of the dolphin's blubber shear compliance and loss tangent values of 1/2, 1, and 2 times the measured loss tangent value would result in nine independent materials for investigation. These nine materials would include the value nature has chosen for the dolphin. Because it is well known that polymer chemists can tailor materials to desired mechanical properties, it is proposed to synthesize materials having these dynamic properties that closely match and encompass the measured values for the dolphin's blubber. These materials shall serve as a basis for the assessment of the role of surface compliance on noise.

FLOW EXPERIMENT

The TBL noise would be measured in an acoustically quiet water tunnel with a known noise background such as the facility at the New London Laboratory of NUSC.⁶⁸ Holographic and laser Doppler techniques should be used to characterize the TBL and the surface motion. For each of the nine materials, a holographic

representation of the surface, a laser Doppler characterization of the TBL, and acoustic spectra would be realized. These measurements would be performed under carefully controlled but varied temperature conditions. In particular, the role of surface compliance on the reduction of drag and noise will be evaluated. Possible delay in the onset of turbulence, the decay of fully developed turbulence, and the magnitude of the acoustic wavenumber spectra as a function of surface compliance will be established. The result of such an experiment will be a definitive and rare set of data for TBL on compliant surfaces whose properties are known and encompass a wide range of compliances.

The water tunnel facility at the New London Laboratory (figures 14 and 15, Schloemer⁵⁹) was specifically designed for TBL noise studies. Particular consideration in the design phase was given to providing acoustic isolation of the test section to minimize acoustic contamination caused by the circulating machinery. Centerline velocities from 9 to 48 knots are achievable in the 3.5-in. inside diameter pipe test section. An alternate rectangular test section with a 4 in. x 12 in. cross-section and a working length of 90 in. can be used over a range of velocities up to 11 knots (Schloemer⁵⁹). Water temperature is controllable over a normal range of 60° to 85° F. This facility is ideally suited for conducting carefully controlled experiments to provide detailed measurements of the TBL noise in the presence of a compliant surface.

Measurements of the fluctuating pressure field characteristics on the wall in the absence of a compliant surface have been extensively investigated with typical flush-mounted piezoelectric ceramic probe hydrophones. In figure 16 (Schloemer⁵⁹) the typical wall pressure spectral density is shown for both high (18.0 ft/s) and low (11.4 ft/s) flow speeds. Also shown are the corresponding acoustic background noise spectra measured with no flow through the rectangular section; the flow is diverted through the alternate circular section, with the machinery operating at the speeds corresponding to those used for the measurements in the rectangular section. Nondimensionalized wall pressure spectra were found (Schloemer⁵⁹) to correspond closely with data obtained in other experiments. Convection velocity data, which are shown in figure 3, exhibit a typical behavior for fully developed TBL flow, as do the normalized magnitudes of the longitudinal and lateral cross-spectral densities, which are shown in figures 6 and 7, respectively. While several attempts have been made in other facilities to identify the wavenumber spectral composition of the wall pressure fluctuations, this has not been done for this facility.

Advanced hydrophone technology that has been under development at the New London Laboratory for several years offers the promise of sensors with improved sensitivity and resolution characteristics. Currently being developed are small flexural disk ceramics and both thin and thick film polymers that can be used to provide hydrophones with electrical and physical properties appropriate for TBL studies. Additionally, such hydrophones could be of a low profile design that would enhance the ability to obtain measurements on and within compliant layers with a minimum of disruptive effects on the layer in the immediate vicinity of the sensor.

Basic measurements of the TBL wall pressure fluctuations dominated by energy at the convective wavenumber will be accomplished by utilizing small flush-mounted probe hydrophones, as shown schematically in figure 17. Autospectral

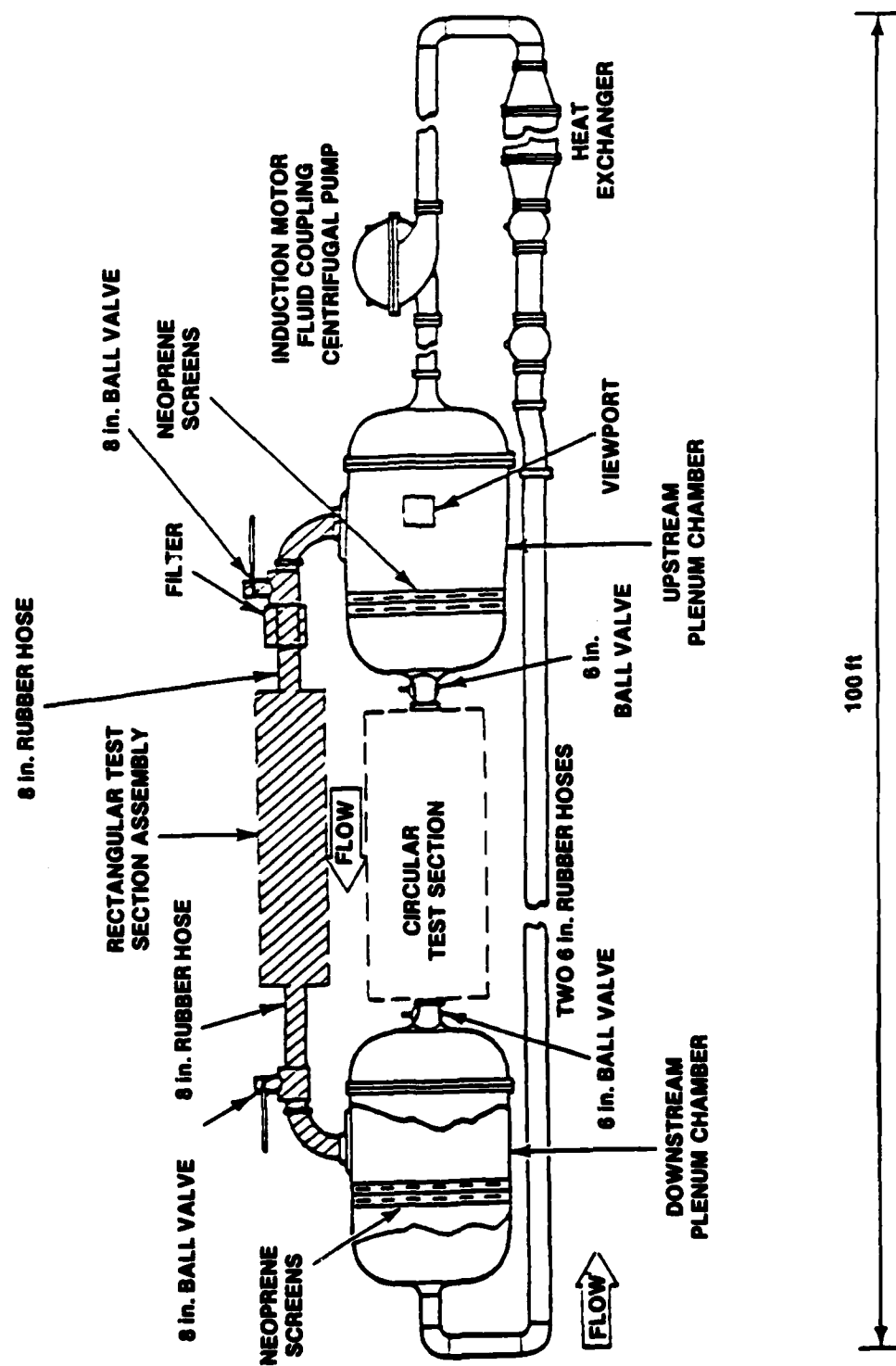


Figure 14. Acoustic Water Tunnel

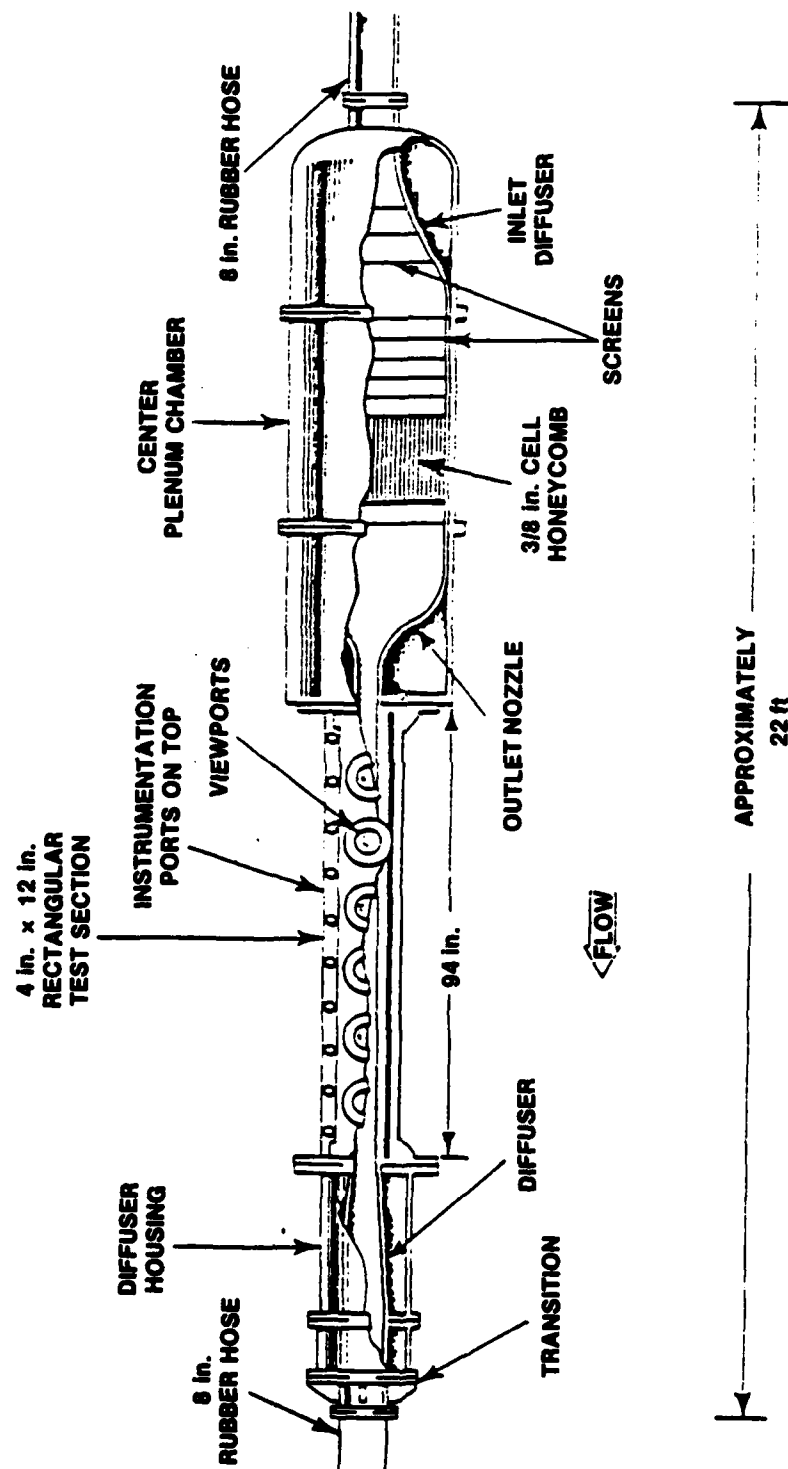


Figure 15. Rectangular Test Section Assembly

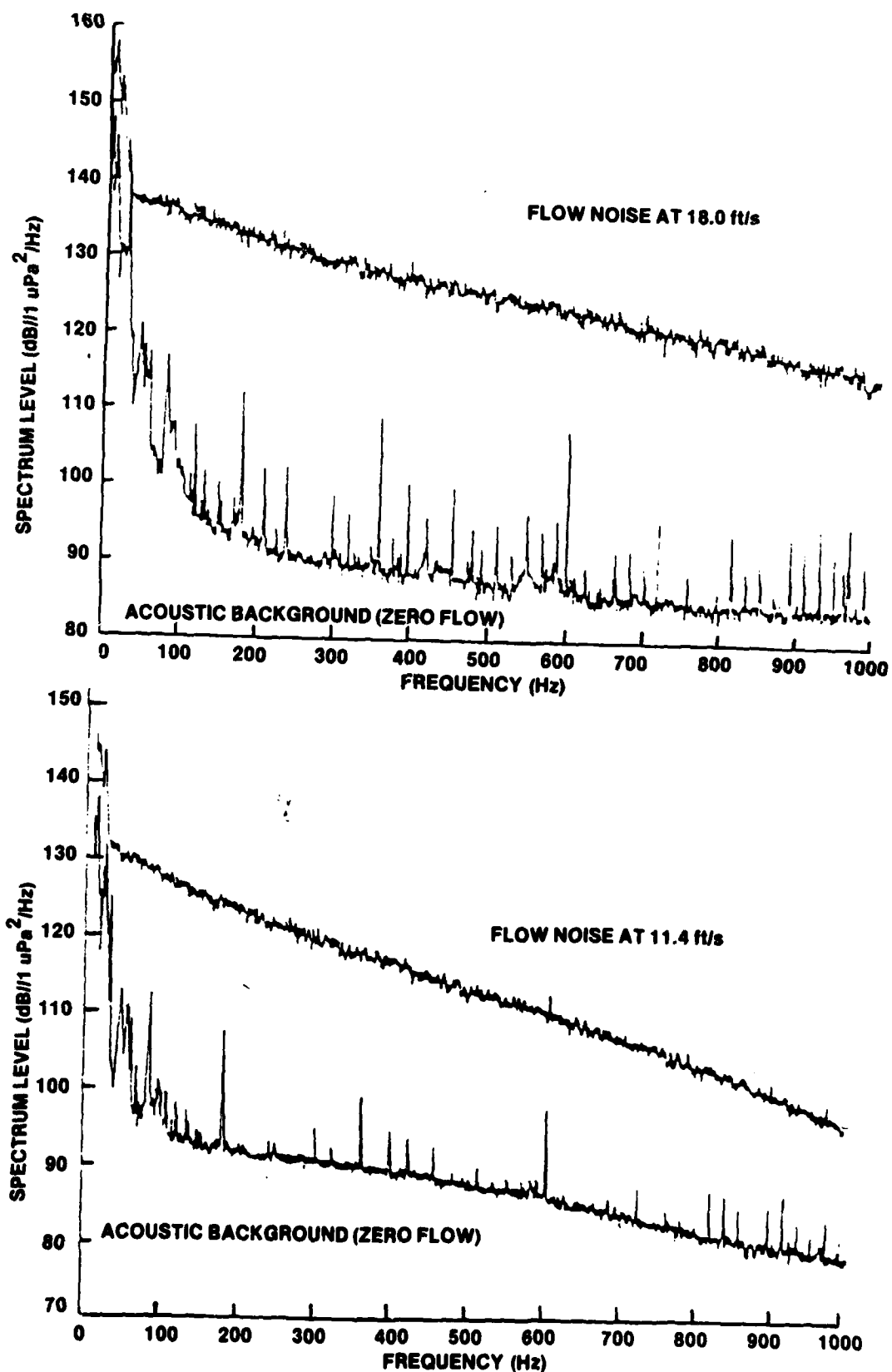


Figure 16. Spectral Density--Background Noise Versus Flow Noise

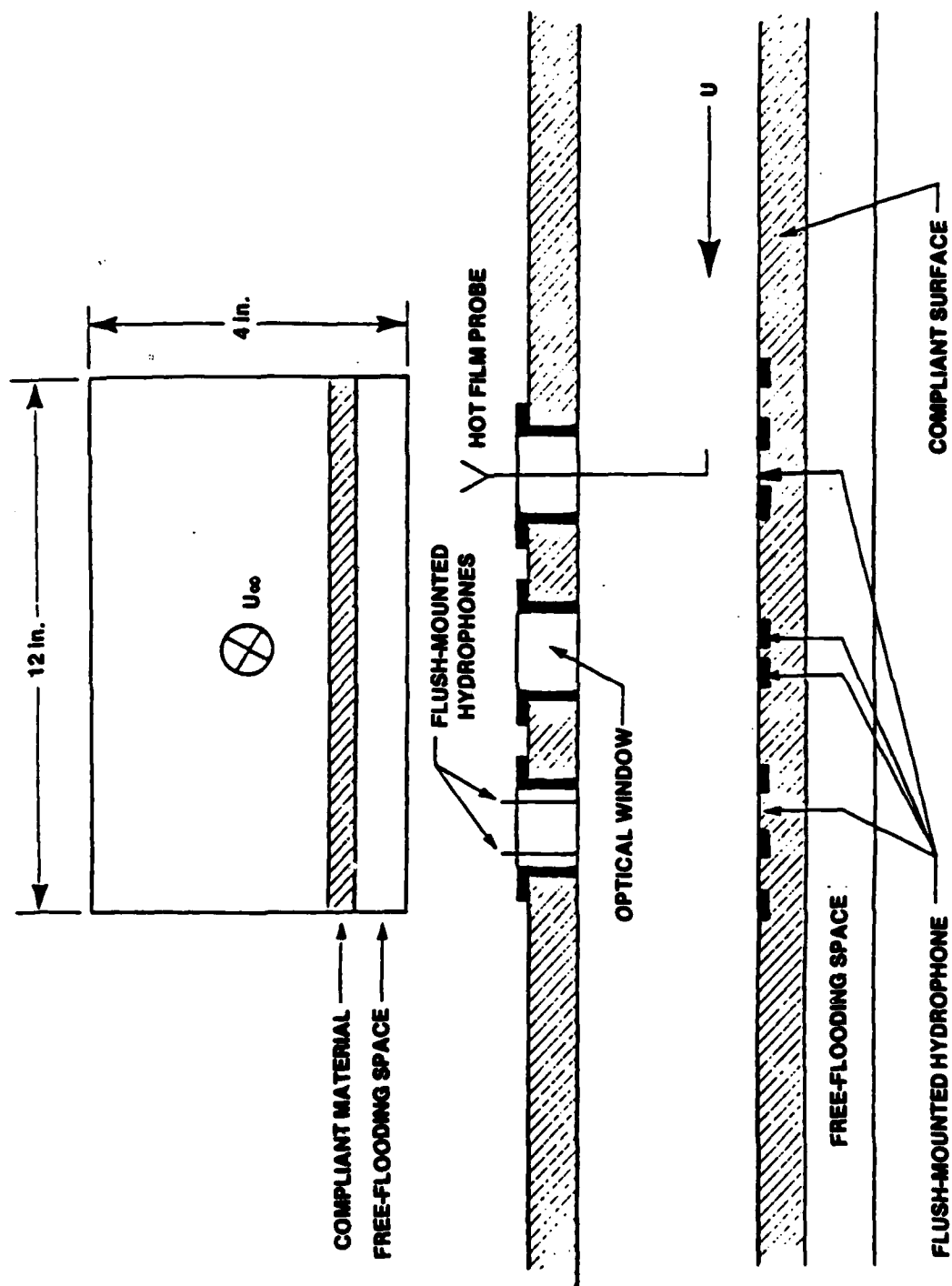


Figure 17. Planned Compliant Surface Experiment

data will permit direct comparison of the convective wavenumber studies with earlier results obtained on bodies of revolution. Appropriate geometric arrangement of several sensors providing selected longitudinal and transverse sensor separation distances will permit detailed cross-spectral analysis of the spatial characteristics of the TBL wall pressure field. Comparison of measurements of various compliant surfaces with a noncompliant surface will be used to quantify and characterize achievable TBL noise reduction. These results will further be compared with results of other drag reduction experiments to note any common physical phenomenon, length scale, etc., that could provide insight into a mechanism for energy dissipation or redistribution. Selection of the specific compliant surfaces for test will be directed by the materials study under this program, although an attempt will be made to include coatings similar to those used in earlier investigations. The initial studies will be conducted in the rectangular test section of the water tunnel at the New London Laboratory, with the compliant material mounted on the lower wall of the test section; this wall serves as a liner for control of the pressure gradient and is easily removed or replaced. Based on an analysis of these results, consideration will be given to the possible need for higher speed tests that might be conducted in the 3.5-in. inside diameter pipe flow section or, following the installation of a higher speed pump, in the rectangular section.

In many practical situations, a structure's response to turbulent flow is maximum at wavenumbers well below the convective range. Measurements of low wavenumber energy for noncompliant surfaces are of basic importance to flow induced noise estimates. Similar measurement for compliant coatings could permit calculating anticipated reductions in flow induced sonar self-noise. Other drag reduction schemes that reduced wall shear stress (τ_w) and convective TBL wall pressure fluctuations ($\overline{P^2}(f)$) have also shown dramatic effects on sonar self-noise. This result suggests that low wavenumber energy, as well as convective energy, may have been altered, although no measurements at the low wavenumbers have yet been made in noise-reduced flows.

In addition to using film sensors and flush-mounted hydrophones, acceleration levels will be measured at each test condition. Fluid temperature will be carefully controlled at selected constant values. Double-pulse holography, a technique developed extensively at the NUSC New London Laboratory, will be employed to effectively "freeze" the motion of the compliant surface. Figure 17 illustrates the optical window that will be used in performance of such measurements. The resultant holograms will be compared to companion velocity-surface motion characterization experiments performed at the NUSC Newport Laboratory water tunnel. This tunnel is equipped with a laser Doppler velocimeter (LDV) and a dye ejection system. The LDV can easily be used to measure velocity profiles and turbulence spectra at any point in the test section.

The planned experiments that have been discussed above are intended not to provide detailed design information but, rather, to quantify the potential of compliant surfaces for Naval noise reduction and determine the value of further efforts in this area.

SUMMARY

This document has reviewed the properties of TBL wall pressure fluctuations. Experimental determination of the power spectra, correlative properties, convection velocities, and wavenumber spectra were summarized. Transducer size effects were discussed as being important at high frequencies and also at low frequencies due to the pressure of the Kline eddies. It was concluded that complete representation of the flow noise spectrum would require a determination of the power as a function of both frequency and wavenumber.

The published data reviewed here suggest that the low wavenumber region of the spectrum includes a component contribution due to the radiated noise that varies in importance as a function of frequency. The high wavenumber region above the convective wavenumber quite likely contains a frequency dependent contribution associated with Kline eddies that should be most pronounced at the lower frequencies. For midrange frequencies, the TBL spectrum has been experimentally characterized largely in terms of the convective wavenumber contribution. However, complete characterization of this spectrum has not been accomplished.

Additionally, this review attempts to highlight the importance of characterization of material properties and suggests a viable technique for determining the complex shear modulus of candidate materials. This review further found that experimental results in noise and drag reduction experiments with compliant surfaces were varied and generally unreproducible. Most probably this variation of experimental results is due to inadequate knowledge of the temperature- and frequency-dependent moduli of the viscoelastic materials tested. A definitive experiment that considers the flow field, the material properties of the surface, the radiated noise field, and the pseudosonic field has been proposed to quantify the role surface compliance plays in the production of TBL noise.

REFERENCES

1. D. Blokhintzev, "The Acoustics of an Inhomogeneous Moving Medium," NACA Technical Memorandum No. 1399, 1956.
2. M. Kramer, "Boundary Layer Stabilization by Distributed Damping," *J. Aero Sciences*, vol. 24, no. 6, 1957.
3. M. J. Lighthill, "On Sound Generated Aerodynamically, I: General Theory," *Proc. Roy. Soc. (London)*, A251, 1952, pp. 564-587; "On Sound Generated Aerodynamically, II: Turbulence as a Source of Sound," *ibid.*, A221, 1954, pp. 1-32.
4. M. J. Lighthill, "Sound Generated Aerodynamically," The Bakerian Lecture, *Proc. Roy. Soc. (London)*, A267, 1962, pp. 147-182.
5. J. E. Ffowcs-Williams, "Sound Radiation From Turbulent Boundary Layers Formed on Compliant Surfaces," *J. Fluid Mech.*, vol. 22, part 2, 1965, pp. 347-358.
6. J. E. Ffowcs-Williams, "The Influence of Simple Supports on the Radiation From Turbulent Flow Near a Plane Compliant Surface," *J. Fluid Mech.*, vol. 26, part 4, 1966, pp. 641-649.
7. J. E. Ffowcs-Williams, "Hydrodynamic Noise," *Annual Review of Fluid Mechanics* (Annual Reviews, Palo Alto, CA), vol. 1, 1969, pp. 197-222.
8. P. Morse and K. V. Ingard, *Theoretical Acoustics*, McGraw Hill Book Company, Inc., NY, 1968.
9. A. Powell, "On the Aerodynamic Noise of a Rigid Flat Plate Moving at Zero Incidence," *J. Acoust. Soc. Am.*, vol. 31, no. 12, 1959.
10. N. Curle, "The Influence of Solid Boundaries Upon Aerodynamic Sound," *Proc. Roy. Soc. (London)*, A231, 1955, pp. 505-514.
11. R. H. Kraichnan, "Pressure Field Within Homogeneous Anisotropic Turbulence," *J. Acoust. Soc. Am.*, vol. 28, no. 1, 1956, pp. 64-72.
12. R. H. Kraichnam, "Pressure Fluctuations in Turbulent Flow Over a Flat Plate," *J. Acoust. Soc. Am.*, vol. 28, no. 3, 1956, pp. 378-390.
13. R. H. Kraichnam, "Noise Transmission From Boundary Layer Pressure Fluctuations," *J. Acoust. Soc. Am.*, vol. 29, no. 1, 1957.

REFERENCES (Cont'd)

14. G. K. Batchelor, "Pressure Fluctuations in Isotropic Turbulence," *Proc. of Cambridge Philosophical Society*, vol. 47, part 2, 1951, pp. 359-374.
15. H. M. Fitzpatrick and M. Strasberg, *Hydrodynamic Sources of Sound*, David Taylor Model Basin Report No. 1269, January 1959.
16. G. P. Haddle and E. J. Skudrzyk, "The Physics of Flow Noise," *J. Acoust. Soc. Am.*, vol. 46, 1969, pp. 130-157.
17. W. W. Willmarth, "Pressure Fluctuations Beneath Turbulent Boundary Layers," *Annual Review of Fluid Mechanics*, vol. 7, 1975, pp. 13-38.
18. D. Ross, *Mechanics of Underwater Noise*, Pergamon Press, NY, 1976, pp. 185-201.
19. M. Harrison, "Pressure Fluctuations on the Wall Adjacent to a Turbulent Boundary Layer," *Second Symposium on Naval Hydrodynamics*, ONR, Dept. of Navy, ACR-38, Washington, DC, 1958, pp. 107-126.
20. W. W. Willmarth, "Wall-Pressure Fluctuations in a Turbulent Boundary Layer," *J. Acoust. Soc. Am.*, vol. 28, 1956, p. 1048.
21. E. Skudrzyk and G. Haddle, "Noise Production in a Turbulent Boundary Layer by Smooth and Rough Surfaces," *Second Symposium on Naval Hydrodynamics Noise Cavity Flow*, ONR, National Academy of Science National Resources Council, Washington, DC, 1958, pp. 78-180.
22. E. Skudrzyk and G. Haddle, "Noise Production in a Turbulent Boundary Layer by Smooth and Rough Surfaces," *J. Acoust. Soc. Am.*, vol. 32, no. 1, 1960, pp. 19-34.
23. T. H. Hodgson, "Pressure Fluctuation in Shear Flow Turbulence," Thesis, Faculty of Engineering, University of London; also Call. Aeronaut., Cranfield Note No. 129, 1962.
24. W. W. Willmarth and C.E. Wooldridge, "Measurements of the Fluctuating Pressure at the Wall Beneath a Thick Turbulent Boundary Layer," *J. Fluid Mech.*, vol. 14, 1962, p. 187.
25. M. K. Bull, *Properties of the Fluctuating Wall Pressure Field of a Turbulent Boundary Layer*, Advisory Group for Aerospace Research and Development, NATO (AGARD) Report No. 455, 1963, pp. 1-34.

REFERENCES (Cont'd)

26. J. S. Serafine, *Wall Pressure Fluctuation and Pressure Velocity Correlations in Turbulent Boundary Layers*, Advisory Group for Aerospace Research and Development, NATO (AGARD) Report No. 747, 1963.
27. W. A. VonWinkle, "Some Measurements of Longitudinal Space Time Correlation of Wall Pressure Fluctuation in Turbulent Pipe Flow," PH.D. Dissertation, University of California, 1960; also W. A. VonWinkle, *Some Measurements of Longitudinal Space-Time Correlations of Wall Pressure Fluctuations in Turbulent Pipe Flow*, USL (now NUSC) Technical Report No. 526, Naval Underwater Systems Center, New London, CT, 17 August 1961.
28. W. A. VonWinkle and G. M. Corcos, "Some Measurements of the Pressure Field at the Boundary of a Fully Developed Pipe Flow," USL (now NUSC) Technical Memorandum No. 1210-187-59, Naval Underwater Systems Center, New London, CT, 28 December 1959.
29. G. M. Corcos, *Pressure Fluctuations in Shear Flows*, University of California, Inst. of Eng. Res. Report, Series 183, No. 2, 1962.
30. H. P. Bakewell, Jr., G. F. Carey, J. J. Libuha, H. H. Schloemer, and W. A. VonWinkle, *Wall Pressure Correlations in Turbulent Pipe Flow*, NUSL (now NUSC) Report No. 559, Naval Underwater Systems Center, New London, CT, 20 August 1962.
31. H. H. Schloemer, *Effects of Pressure Gradients on Turbulent-Boundary-Layer Wall-Pressure Fluctuations*, NUSL (now NUSC) Technical Report No. 747, Naval Underwater Systems Center, New London, CT, 1 July 1966.
32. H. H. Schloemer, "Effects of Pressure Gradients on Turbulent-Boundary-Layer Wall-Pressure Fluctuations," *J. Acoust. Soc. Am.*, vol. 42, 1967, pp. 93-113.
33. M. K. Bull, "Wall-Pressure Fluctuations Associated With Subsonic Turbulent-Boundary Layer Flow," *J. Fluid Mech.*, vol. 28, 1967, pp. 719-754.
34. W. K. Blake, *Turbulent Boundary Layer Wall Pressure Statistics on Smooth and Rough Walls*, MIT Department of Naval Architecture and Marine Engineering, Acoustics, & Vibration Laboratory Report No. 70208-1, January 1969; also *J. Fluid Mech.*, vol. 44, 1970, pp. 637-660.

REFERENCES (Cont'd)

35. W. A. VonWinkle, "An Evaluation of a Boundary Layer Stabilization Coating," USL (now NUSC) Technical Memorandum No. 922-111-61, Naval Underwater Systems Center, New London, CT, 15 May 1961.
36. H. P. Bakewell, Jr., "Turbulent Wall-Pressure Fluctuations on a Body of Revolution," *J. Acoust. Soc. Am.*, vol. 43, no. 6, 1961, pp. 1358-1363.
37. Private communication: G. F. Carey et al. and Dr. W. A. Von Winkle.
38. W. W. Willmarth, "Corrigendum: Measurements of the Fluctuating Pressure at the Wall Beneath a Thick Turbulent Boundary Layer," *J. Fluid Mech.*, vol. 21, part 1, 1965, pp. 107-109.
39. M. K. Bull and J. L. Willis, *Some Results of Experimental Investigations of the Surface Pressure Field Due to a Turbulent Boundary Layer*, University of Southampton AASU Report No. 199, 1961.
40. W. W. Willmarth, N.A.S.A. Memo 3-17-59W, 1959.
41. W. W. Willmarth and F.W. Roos, "Resolution and Structure of the Wall-Pressure Field Beneath a Turbulent Boundary Layer," *J. Fluid Mech.*, vol. 22, 1965, pp. 81-94.
42. B. D. Mugridge, "Turbulent Boundary Layers and Surface Pressure Fluctuations On Two-Dimensional Aerofoils," *J. Sound and Vibr.*, vol. 18, 1971, pp. 475-486.
43. I. F. Kadykov and L. M. Lyamshev, "Influence of Polymer Additives on the Pressure Fluctuations in a Boundary Layer," *Sov. Phys. Acoust.*, vol. 16, 1970, pp. 59-63.
44. B. A. Toms, "Some Observations on the Flow of Linear Polymer Solutions Through Straight Tubes at Large Reynolds Numbers," *Proc. Fifth Inter. Cong. on Rheology*, North Holland Publ. Co., Amsterdam, 1948, pp. 135-141.
45. A. G. Fabula, "The Toms Phenomenon in Turbulent Flow of Very Dilute Polymer Solutions," *Proc. Fourth Mtg. Congr. on Rheology*, Interscience Publ., NY., 1965, pp. 455-479.

REFERENCES (Cont'd)

46. E. R. Von Driest "Turbulent Drag Reduction of Polymeric Solutions," *J. Hydronautics*, vol. 4, 1976, pp. 120-126.
47. G. M. Corcos, "Resolution of Pressure in Turbulence," *J. Acoust. Soc. Am.*, vol. 35, 1963, pp. 192-199.
48. R. B. Gilchrist and W. A. Strawderman, "Experimental Hydrophone-Size Correction Factor for Boundary-Layer Pressure Fluctuations," *J. Acoust. Soc. Am.*, vol. 38, 1965, pp. 298-302.
49. L. M. Lyamshev and S. A. Salosina, "Influence of Pickup Dimensions on the Measurements of the Spectrum of Wall-Pressure Fluctuations in a Boundary Layer," *Sov. Phys. Acous.*, vol. 12, 1966, pp. 228-229.
50. F. E. Geib, Jr., "Measurements on the Effect of Transducer Size on the Resolution of Boundary-Layer Pressure Fluctuations," *J. Acoust. Soc. Am.*, vol. 6, 1969, pp. 253-261.
51. W. W. Willmarth, NACA Technical Note No. 4139, 1958.
52. H. P. Bakewell, Jr., and J. L. Lumley, "Viscous Sublayer and Adjacent Wall Region in Turbulent Pipe Flow," *Phys. Fluids*, vol. IV, no. 9, 1967, pp. 1880-1889.
53. S. J. Kline, W. C. Reynolds, and P. W. Runstadler, *An Experimental Investigation of the Flow Structure of the Turbulent Boundary Layer*, Department of Mechanical Engineering, Stanford University, Stanford, CA, 1963.
54. S. J. Kline and F. A. Schraub, *A Study of the Structure of the Turbulent Boundary Layer With and Without Longitudinal Pressure Gradients*, Department of Mechanical Engineering, Stanford University, Stanford, CA, Report MD-12, 1965.
55. R. Emmerling, *The Instantaneous Structure of the Wall-Pressure Under a Turbulent Boundary Layer Flow*, Max Planck-Institut für Stromungsforschung Report No. 9, 1973.
56. M. K. Bull and A. S. W. Thomas, "High Frequency Wall-Pressure Fluctuations in Turbulent Boundary Layers," *Phys. Fluids*, vol. 19, no. 4, April 1976, pp. 597-599.

REFERENCES (Cont'd)

57. A. Dinkelacker, M. Hessel, G. Meier, and G. Scheure, "Investigation of Pressure Fluctuations Beneath a Turbulent Boundary Layer by Means of an Optical Method," *Phys. Fluids*, vol. 20, no. 10, part II, October 1977, pp. 216-224.
58. F. M. White, *A Unified Theory of Wall Pressure Fluctuations*, NUSL (now NUSC) Report No. 629, Naval Underwater Systems Center, New London, CT, 1 December 1964; and S. Gardner, "On Surface Pressure Fluctuations Produced by Boundary Layer Turbulence," *Acustica* vol. 16, no. 2, 1965/1966, pp. 67-74.
59. H. H. Schloemer, *Installation of a Rectangular Test Section for Acoustic Water Tunnel Studies of Flow-Induced Noise*, NUSC Technical Report No. 4763, Naval Underwater Systems Center, New London, CT, 21 August 1974.
60. F. W. Boggs and N. Tokita, "A Theory of the Stability of Laminar Flow Along Compliant Plates," *Third Symposium on Naval Hydrodynamics, High Performance Ships, 19-22 September 1960*, ACR-65, ONR, Washington, DC.
61. W. A. VonWinkle and J. E. Barger, "An Evaluation of a Boundary Layer Stabilization Coating," USL (now NUSC) Problem 1-612-00-00, Naval Underwater Systems Center, New London, CT, 15 May 1961. Presented at the *Sixty-First Meeting of the Acoustical Society of America, Philadelphia, PA*, 10 May 1961.
62. V. Babenko, "Certain Mechanical Characteristics of Dolphin Skin," *Bionika*, vol. 5, 1971, pp. 76-81.
63. V. Babenko and M. Surkina, "Determination of the Oscillating-Mass Parameter of the Integuments of Certain Sea Creatures," *Bionika*, vol. 5, 1971, pp. 94-98.
64. W. S. Cramer, *Measurement of the Acoustic Properties of Solid Polymers*, Naval Ship Research and Development Center SAD-472-1945, June 1972.
65. D. J. Solarek, Jr., "Dynamic and Transient Characteristics of Rubberlike Materials: A Survey," Naval Undersea Center (NUC) TN 917, August 1972.
66. W. M. Carey, R. Doolittle, et al., *Dynamic Properties and Towed Array Materials*, MAR, Inc., Technical Report 143, May 1975.

REFERENCES (Cont'd)

67. E. K. Fitzgerald and J. D. Ferry, *Method for Determining the Dynamic Mechanical Behavior of Gels and Solids at Audio Frequencies; Comparison of Mechanical and Electrical Properties*, Department of Physics and Chemistry, University of Wisconsin, June 1952; also *J. Collaid, Sci.*, vol. 8. no. 1, February 1953, pp. 1-34.
68. G. F. Carey, J. E. Chlupsa, and H. H. Schloemer, "Acoustic Turbulent Water-Flow Tunnel," *J. Acoust. Soc. Am.*, vol. 41, no. 2, 1967, pp. 373-379.

Initial Distribution List

| ADDRESSEE | NO. OF COPIES |
|---|---------------|
| CINCLANTFLT | 1 |
| CINCPACFLT | 1 |
| COMSECONDFLT | 1 |
| COMTHIRDFLT | 1 |
| COMSIXTHFLT | 1 |
| COMSEVENTHFLT | 1 |
| COMASWFORSIXTHFLT | 1 |
| COMSUBLANT | 1 |
| COMSUBPAC | 1 |
| COMOPTEVFOR | 1 |
| COMSUBRON 1, 2, 3, 4, 6, 7, 8, 10, 14, 15, 16, 18 | 12 |
| COMSUBGRU 5, 7 | 2 |
| COMSUBDEVGRUONE | 1 |
| COMSUBDEVRON 12 | 1 |
| ASN (RE&S), (G. A. Cann) | 1 |
| Deputy USDR&E (Res & Adv Tech) | 1 |
| Deputy USDR&E (Dir Elect & Phys Sc) | 1 |
| OASN, Spec Dep for Adv Concept, Dep Assist Secretary (Systems), Dep Assist Secretary (Res & Adv Tech) | 3 |
| ONR-100, -102, -200, -220, -400, -410, -420, -422, -425, -425, -425AC, -430 | 12 |
| CNO. OP-02, -095, -21, -211, -22, -951, -951D, -951E, -952, -96, -981, -983 | 12 |
| CNM, MAT-00, -05, ASW-10, -13, SP-20 | 5 |
| Systems Project Office (PM-2) Trident | 1 |
| DIA, DT-2C | 1 |
| NRL, 5100, 5160, 5162 (W. Carey), 2620 (Library) | 4 |
| NORDA-110 (R. Martin), -300 (H. Eppert), -335 (A. Pressman), -350 (J. McCaffrey), -500 (L. Solomon), -520 (C. Staurt) (CDR McAllister) (R. Gardner), -530 (E. Chaika) | 9 |
| SUBBASE LANT | 1 |
| OCEANAV | 1 |
| NAVOCEANO | 1 |
| NAVELECSYSCOM, PME-124, -30, -140, -160, ELEX-320 | 5 |
| NAVSEASYSYSCOM, SEA-003, -05, -05H, -05R, -06, -06R, -62, -62R, -63, -63R, -63R-1, -63X, -631Y, -63Z, -92, -92R | 16 |
| PMS-402, -406, -393, -395 | 4 |
| NAVAIRDEVCON | 1 |
| NOSC, 711, 7112, 7121, 7122, Library (Code 6565) | 5 |
| NAVWPNSCEN | 1 |
| NCSC | 1 |
| CIVENGRLAB | 1 |
| NAVSURFWPNCEN, White Oak Lab | 2 |
| DWTNSRDC, ANNA, BETH | 2 |
| NISC | 1 |
| NAVPGSCOL | 1 |
| NAVWARCOL | 1 |
| APL/UW, Seattle | 1 |
| ARL/PENN STATE, State College | 1 |
| DTIC | 2 |
| DARPA | 1 |
| NATIONAL RESEARCH COUNCIL | 1 |
| WOODS HOLE OCEANOGRAPHIC INSTITUTION | 1 |
| ENGINEERING SOCIETIES LIB, UNITED ENGRG CIR | 1 |
| ARL/ UNIV OF TEXAS | 1 |
| MARINE PHYSICAL LAB, SCRIPPS | 1 |
| MAR, INC (H. Bakewell) | 1 |
| ANALTECHNS (T. Dziedzic) | 1 |
| EDOCORP (J. Vincenzo) | 1 |
| OPERRES, INC. (Dr. V. P. Simmons) | 1 |
| B-K DYNAMICS (J. Fitzgerald) | 1 |
| TRACOR (J. Gottwald) (W.W. Williams) | 2 |